

PROYECTO FIN DE CARRERA

TEMA: Evaluación de la absorción dependiente del ángulo.

TÍTULO: Evaluation of angle-dependent absorption: Computer simulation and listening test for an objective and subjective evaluation.

AUTOR: David Vázquez Rufino

TUTOR: Sönke Pelzer

DEPARTAMENTO: *Institut für Technische Akustik der RWTH Aachen*

CENTRO DE LECTURA: *Institut für Technische Akustik der RWTH Aachen*

Fecha de Lectura: 22 de agosto de 2013

Calificación: 1,3

RESUMEN DEL PROYECTO:

El objetivo de este trabajo es la evaluación objetiva y subjetiva del coeficiente de absorción en función del ángulo de incidencia de la onda de sonido. La suposición de un coeficiente de absorción constante con respecto al ángulo de incidencia no siempre se sostiene. Por ello, un nuevo modelo considerando la reflexión dependiente del ángulo se debe tener en cuenta para obtener predicciones más certeras en el campo del sonido. El estudio proporciona información sobre el comportamiento de diferentes materiales en distintos recintos, dependientes del modelo de reflexión de las ondas de sonido incidentes.

Debido a las dificultades a la hora de realizar las medidas y, por lo tanto, a la falta de datos, los coeficientes de absorción dependientes del ángulo a menudo no se tienen en cuenta a la hora de realizar las simulaciones. Hoy en día, aún no hay una tendencia de aplicar el coeficiente de absorción dependiente del ángulo para mejorar los modelos de reflexión. Por otra parte, para una medición satisfactoria de la absorción dependiente del ángulo, sólo hay unos pocos métodos. Las técnicas de medición actuales llevan mucho tiempo y hay algunos materiales, condiciones y ángulos que no pueden ser reproducidos y, por lo tanto, no es posible su medición. Sin embargo, en el presente estudio, los ángulos de incidencia de las ondas de sonido son conocidos y almacenados en una de base de datos para cada uno de los materiales, de modo que los coeficientes de absorción para el ángulo dado pueden ser devueltos siempre que sean requeridos por el usuario.

Para realizar el estudio se llevó a cabo una evaluación objetiva, por medio de la implementación del factor de reflexión dependiente del ángulo en los modelos de fuentes imagen y trazado de rayos. Los resultados fueron analizados después de ser comparados con el promedio de los datos obtenidos en medidas en el campo difuso. La simulación se hizo una vez se configuraron un número de materiales creados por el autor, a partir de los datos existentes en la literatura y los catálogos de fabricantes. Los modelos de Komatsu y Mechel sirvieron como referencia para los materiales porosos, configurando la resistividad al aire o el grosor, y para los paneles perforados, introduciendo el radio de los orificios y la distancia entre centros, respectivamente. Estos materiales se situaban en la pared opuesta a la que se consideraba que debía alojar a la fuente sonora. El resto de superficies se modelaban con el mismo material, variando su coeficiente de absorción y/o de dispersión. Al mismo tiempo, una serie de recintos fueron modelados para poder reproducir distintos escenarios de los que obtener los resultados.

Sin embargo, los cambios en las características acústicas de un recinto no significan variaciones en la percepción por parte del oyente. Por ello, una evaluación subjetiva adicional permitió una comparación entre los diferentes resultados obtenidos mediante la simulación informática y la respuesta de los individuos que participaron en la prueba de escucha. Ésta fue diseñada bajo las pautas del modelo de test *three-alternative forced-choice* (3AFC), con treinta y dos preguntas diferentes. En cada iteración los sujetos fueron preguntados por una secuencia alterna entre tres señales, siendo dos de ellas iguales. Éstas podían ser tanto ráfagas de ruido rosa como señales naturales, en este test se utilizó un fragmento de una obra clásica interpretada por un piano. Antes de contestar al cuestionario, los bloques de preguntas eran ordenados al azar. Para cada ensayo, la mezcla era diferente, así los sujetos no repetían la misma prueba, evitando un sesgo por efectos de aprendizaje. Los bloques se barajaban recordando siempre el orden inicial, para después almacenar los resultados reordenados. La prueba de escucha fue realizada por veintitrés personas, toda ellas con conocimientos dentro del campo de la acústica. Antes de llevar a cabo la prueba de escucha en un entorno adecuado, una hoja con las instrucciones fue facilitada a cada persona. Los resultados muestran la influencia y percepción de las dos maneras distintas de implementar las reflexiones de una superficie –ya sea con respecto a la propiedad de difusión o de absorción dependiente del ángulo de los materiales.

Los resultados objetivos, después de ejecutar las simulaciones, muestran los datos medios obtenidos para comprender el comportamiento de distintos materiales de acuerdo con el modelo de reflexión utilizado en el caso de estudio. En las tablas proporcionadas en la memoria se muestran los valores del tiempo de reverberación, la claridad y el tiempo de caída temprana. Los datos de las características del recinto obtenidos en este análisis tienen una fuerte dependencia respecto al coeficiente de absorción de los diferentes materiales que recubren las superficies del cuarto.

En los resultados subjetivos, la media de percepción, a la hora de distinguir las distintas señales, por parte de los sujetos, se situó significativamente por debajo del umbral marcado por el punto de inflexión de la función psicométrica. Sin embargo, es posible concluir que la mayoría de los individuos tienden a ser capaces de detectar alguna diferencia entre los estímulos presentados en el 3AFC test.

En conclusión, la hipótesis de que los valores del coeficiente de absorción dependiente del ángulo difieren es contrastada. Pero la respuesta subjetiva de los individuos muestra que únicamente hay ligeras variaciones en la percepción si el coeficiente varía en intervalos pequeños entre los valores manejados en la simulación. Además, si los parámetros de los

materiales acústicos no son exagerados, los sujetos no perciben ninguna variación. Los primeros resultados obtenidos, proporcionando información respecto a la dependencia del ángulo, llevan a una nueva consideración en el campo de la acústica, y en la realización de nuevos proyectos en el futuro.

Para futuras líneas de investigación, las simulaciones se deberían realizar con distintos tipos de recintos, buscando escenarios con geometrías irregulares. También, la implementación de distintos materiales para obtener resultados más certeros. Otra de las fases de los futuros proyectos puede realizarse teniendo en cuenta el coeficiente de dispersión dependiente del ángulo de incidencia de la onda de sonido. En la parte de la evaluación subjetiva, realizar una serie de pruebas de escucha con distintos individuos, incluyendo personas sin una formación relacionada con la ingeniería acústica.

Abstract

The aim of this thesis is the subjective and objective evaluation of angle-dependent absorption coefficients. As the assumption of a constant absorption coefficient over the angle of incidence is not always held, a new model acknowledging an angle-dependent reflection must be considered, to get a more accurate prediction in the sound field. The study provides information about the behavior of different materials in several rooms, depending on the reflection modeling of incident sound waves.

An objective evaluation was run for an implementation of angle-dependent reflection factors in the image source and ray tracing simulation models. Results obtained were analysed after comparison to diffuse-field averaged data. However, changes in acoustic characteristics of a room do not always mean a variation in the listener's perception. Thus, additional subjective evaluation allowed a comparison between the different results obtained with the computer simulation and the response from the individuals who participated in the listening test. The listening test was designed following a three-alternative forced-choice (3AFC) paradigm. In each interaction asked to the subjects a sequence of either three pink noise bursts or three natural signals was alternated. These results were supposed to show the influence and perception of the two different ways to implement surface reflection –either with diffuse or angle-dependent absorption properties. Results show slightly audible effects when material properties were exaggerated.

Contents

1. Introduction	11
2. State of the art.....	13
3. Theoretical background	15
3.1. Definitions	15
3.2. Measuring methods.....	16
3.3. Angle-dependent absorption coefficient.....	17
3.4. Non-locally reacting materials.....	18
3.5. Room acoustics simulation	19
3.5.1. Image source model	19
3.5.2. Stochastic ray tracing	19
3.5.3. Auralization.....	19
3.6. Listening test.....	20
3.6.1. Test setup: three-alternative forced-choice	20
4. Application of angle-dependent absorption coefficient in room acoustics simulations	23
4.1. Example rooms and example materials	23
4.2. Binaural room impulse response simulation, <i>RAVEN</i> and auralization	28
4.3. Analyzed room acoustics parameters.....	28
4.4. Conducting the listening test.....	29
5. Discussion of results.....	33
5.1. Room acoustic parameters results.....	33
5.2. Listening test results	43
6. Conclusion.....	47
Appendix A	49
Appendix B.....	51
Bibliography	53

Figures index

Figure 1: Screenshot of the interface used in the listening test by subjects. There are three buttons to replay the sample, when needed, and a text field where any comment could be given.....	21
Figure 2: Box-shaped room. Screen capture from the Sketch up model used as the example room, which size is 15x7x4. The absorber wall was placed in the small wall (7x4) seen on the left side of the picture.	24
Figure 3: Alternative example rooms for future simulations.	24
Figure 4: <i>ita_impcalc_gui interface</i> . The screenshot shows the different options at the time the user wants to create a new material with different layers.....	25
Figure 5: Sketch of the layered materials. In order: Material 1, Material 2 and Material 3 explained in the previous paragraph.....	26
Figure 6: Polar diagram corresponding to the second material composed of Basalt wool-Air-Perforated plate (Material 1).....	26
Figure 7: Polar diagram corresponding to the second material composed of Perforated plate-Air-Basalt wool (Material 2).	27
Figure 8: Polar diagram corresponding to the second material composed of Porous material-Air-Basalt wool-Thick air-Perforated plate-Thin air (Material 3).	27
Figure 9: Results for the reverberation time for the different cases with zero scattering. Each graphic put together the angle-dependent (blue line) and diffused averaged (green line) modeling of the rear absorber with applied material. On the ordinate axe is represented the Reverberation time (T_{30}). On the abscissa axe shows the frequency in Hertz.	39
Figure 10: Results for the different cases with a scattering value of 0.2. Each graphic put together the angle-dependent (blue line) and diffused averaged (green line) modeling of the rear absorber with applied material. On the ordinate axe is represented the Reverberation time (T_{30}). On the abscissa axe shows the frequency in Hertz.	42
Figure 11: Lecture hall with a volume of 2200 m ³ . The orange wall shows where the materials were employed.....	43
Figure 12: Objective results of the lecture hall showing differences between diffuse and angle-dependent modeling of the rear wall absorber with applied material 2. Remaining walls were set to 15% absorption and 20% scattering.....	44
Figure 13: Objective results of the lecture hall showing differences between diffuse and angle-dependent modeling of the rear wall absorber with applied material 4. Remaining walls were set to 15% absorption and 20% scattering.....	45

- Figure 14:** Results of the listening test with detection rates on the ordinate. On the left are the detection rates of all 23 participants. On the right all results are averaged. The median lies significantly below the 67%-point of the detection range. 46
- Figure 15:** Results of the listening test with detection rates on the ordinate. On the left are the four different materials A, B, C and D. On the right are two different absorption coefficients (left: 30% vs right: 15%). 46
- Figure 16:** Results of the listening test with detection rates on the ordinate. On the left are two different scattering coefficients (left: 0% vs. right: 20%). On the right are two different signals (left: pink noise bursts vs. right: piano). 46
- Figure 17:** 6.25 Length-related Airflow resistivity in different layers of insulation. 6.55 Specific Airflow resistivity of loose optical fibers, multiple fiber diameter as a function of density. 6.56 Specific Airflow resistivity of fibers. 1 cotton, 2 PC-Fibers; 3 mineral fiber, 2 ... 10 μm ; 4 basalt wool, 2 ... 8 μm ; 5 aluminum wool, 7 μm 49
- Figure 18:** Strömungsresistenz Ξ verschiedener Fasermaterialien als Funktion des Raumgewichts RG; Meßpunkte und Regressionsgeraden. 50

Tables index

Table 1: Average results of T_{30} changing the rear wall applying the angle-dependent reflection and diffuse-average values of the three materials used for the simulation. The scattering value is constantly ($\alpha = 0.02$).....	33
Table 2: Average results of C_{50} changing the rear wall applying the angle-dependent reflection and diffuse-average values of the three materials used for the simulation. The scattering value is $\alpha = 0.02$	34
Table 3: Average results of EDT changing the rear wall applying the angle-dependent reflection and diffuse-average values of the three materials used for the simulation. The scattering value is $\alpha = 0.02$	34
Table 4: Average results of T_{30} changing the rear wall applying the angle-dependent reflection and diffuse-average values of the three materials used for the simulation. The scattering value is $\alpha = 0.2$	34
Table 5: Average results of C_{50} changing the rear wall applying the angle-dependent reflection and diffuse-average values of the three materials used for the simulation. The scattering value is $\alpha = 0.2$	35
Table 6: Average results of EDT changing the rear wall applying the angle-dependent reflection and diffuse-average values of the three materials used for the simulation. The scattering value is $\alpha = 0.2$	35
Table 7: Composition, size, characteristics and thickness of the first material describe in point 3.5.4.....	51
Table 8: Composition, size, characteristics and thickness of the second material describe in point 3.5.4.	51
Table 9: Composition, size, characteristics and thickness of the third material describe in point 3.5.4.....	52

1. Introduction

Due to complicated measurements and thus a lack of data, angle-dependent absorption coefficients are often neglected in simulations. Nowadays, there is still no tendency of implementing angle-dependent absorption coefficient to improve reflecting models. Moreover, for a successful measurement of angle-dependent absorption, there are only a few approaches [1]. Current measurement techniques take a long time and there are some materials, conditions and angles that cannot be measured [2]. Therefore, the purpose of this bachelor thesis is the investigation of the changes in the reflection modeling and the way an individual perceives these variations in a room.

It is possible to derive angle-dependent data assuming a certain angular behaviour. Then, the full polar data is extrapolated after measuring a single angle, according to an expected reaction of the material property. Furthermore, after reverberation room diffuse field measurements, it is possible to reconstruct angle-dependent data [3] [4]. Nowadays, research in this area has led to various approaches to measure the absorption coefficient. There are several methods, not all of them standardized, which assume that environmental conditions do not change between one trial and the next one, to measure absorption characteristics in materials: (1) the free field method, (2) the impedance tube method and (3) a number of non-standardized *in-situ* models. The impedance tube method is limited in its application to normal incidence input, not allowing oblique incidence measurements. Therefore, the need of a method for oblique incident sound allowing angle-dependent absorption data is found in the free field method, concretely in the two microphone measurement way. As major drawback, it needs large samples, which can be difficult to produce. Only in case of locally reacting materials, this provides a valid result. *In-situ* models allow the determination of the true absorption properties of materials in their final use conditions for measurements or simulations [5].

As the required data cannot be easily obtained with these common techniques, the remaining option is a combination of the simulated data with an example surface, based on the Komatsu model [2], and the *in-situ* measurement. The Komatsu model uses material's airflow resistivity and thickness to calculate angle-dependent absorption coefficients of porous materials. In the concrete case of this work, different materials were layered on top of each other [6].

In software engineering, generally, the accuracy of calculation is hard to estimate and depends on numerous external parameters of the software [7]. Specifically, for computer simulation of sound propagation in rooms, realistic results are obtained when not only specular reflections are considered, but also diffuse reflections, especially when irregularities of wall surfaces are neither small nor large compared to the wavelengths [8]. However, results strongly depend on the location of the source and the receiver, making these valid only for a given source-receiver situation. The evaluation of results is based on the impulse response, predicted with image source and ray tracing

algorithms. According to the different literature, the main reason to use ray tracing is that approximations using theories of reverberation (e. g. based on Fitzroy's and Arau-Puchades formula) do not work adequately in all situations [9]. In a room with regular shape and non-uniform absorption, the effect of surface scattering can be prominent. In the present study, angles of incidence of sound waves are known and can be given to a material database reader so that the absorption coefficients for the given angle can be returned.

The goal of this thesis is to assess the importance of the behaviour of materials for different angles of incidence of the sound waves. Evaluations of the room are done with computer simulations. To compared these objective changes in the simulation results, clarity, reverberation time and early decay time are taken into account. Besides, the evaluator should not forget, that even when there are changes in the properties of the material, subjective perception may not be altered, because it depends on each individual. Thus, a subjective evaluation is carried out.

2. State of the art

Materials' reflection properties can change depending on the angle of incidence of the sound wave. There are four incidence metrics to characterize acoustical surfaces: absorption, diffusion and scattering coefficient [10] and the impedance, being relevant to this work the behaviour of materials in a room according to the first feature. This section will, therefore, focus on different methods to measure angle-dependent absorption coefficient of a surface.

First approaches were the measurements for the absorption coefficient made by means of intensity measurements in steady-state acoustic field conditions by D. Stanzial and A. Fuschini [11] and F. V. Hunt [12]. Hunt obtained the absorption coefficient as functions of both frequency and angle of incidence, yielding, in a small model chamber, different modes of vibration. But owing to the lack of angle-dependent data in the results, these models are no longer in use. To find reliable methods, the following part draws attention to the latest literature.

As the preceding methods mentioned are not as accurate as measurements required, there are two different kinds of models to improve the task. First of all, measuring methods that are directly measures of the angle absorption coefficient. The main disadvantage is the long time it takes to get all the results. Secondly, models give the output data from average data calculated. According to these two statements, there are several ways of obtaining results. Yuzawa [13] presented a method which makes it possible to obtain the absorption coefficient of a wall material by means of an on-the-spot field measurement. The reflection from a sample can be obtained by combining the outputs from two non-directional microphones through a phase inverter, and how, by comparing it with direct sound measured separately, the sound absorption coefficient can be estimated. To obtain the single reflection, a burst tone technique is used, while Yuzawa's measurement technique is used to cancel the incident sound wave. Results are extrapolated from average data, turning out to be non-reliable.

Nonetheless, Mommertz developed an analysis taking under consideration an impulse-shaped signal reflected from the surface, using a reflection or impulse -echo as input data. The improvement was produced in the reflection method by applying a subtraction technique in combination with digitally pre-emphasized pseudo-noise signals, allowing the frequency dependent complex reflection and absorption coefficients to be determined at almost arbitrary angles of sound incidence [14]. According to Mommertz's model, the translation from a set of angle-dependent free field absorption coefficient to a random incidence value is normally carried out using Paris' formula.

It is important, at this point, to introduce the *in-situ* sound absorption coefficient as the sound absorption coefficient for a specified angle of incidence for *in-situ* structure in a semi-anechoic field [15]. The reference work is the improvement of the Delany-Balzley and Miki models to predict acoustical properties in materials written by Komatsu [2], which turns out to be more effective than the conventional models.

A different measurement method to be considered is the Local Plane Wave (LPW) method, which objective is to determine the effective area-average sound absorption coefficient $\alpha_{\text{LPW}}(\mathbf{w})$ of a measurement surface \mathbf{S}' at a distance \mathbf{d} from the material surface \mathbf{S}_m . The LPW is capable of estimating the incident sound intensity without a prior knowledge of the sound field. Therefore, an overall sound field model is not required. It has been reported that free field method are used to measure the normal impedance and the absorption coefficient [16], but for surfaces with angle-dependent impedance, this procedure is not sufficient. It consists of determining the magnitude and the phase of the pressure at the material's surface.

Simulation procedures frequently rely on the premise of diffuse incidence, as a result of the limited information about diffuse absorption coefficients or normal incidence reflection factors provided by the DIN/ISO-standardized methods [17] [18] [19]. In order to get valid results, an improvement of Spandöck's technique is used nowadays [10]. Also, a Fourier-transform post-processing applied to the sound pressures in different distances can be used [20].

Furthermore, for statistical simulation models, such as ray tracing, not only absorption but also scattering performance is an important characteristic [21]. The idea is based on the combination of geometrical and statistical models, in which sound particles are considered to propagate geometrically and the decay process is calculated using the probability of absorption and the mean free path.

In this study, the acoustic simulation is performed with *RAVEN*¹, extended to angle-dependent absorption coefficient, and *ITA_toolbox*² for *Matlab*, using Komatsu model's premises for creating angle-dependent and diffused materials with the function *ita_impcalc_gui* and layered materials after using Mechel's models [6].

¹ *RAVEN* is a software developed by the *Institut für Technische Akustik* (ITA), RWTH Aachen University.

² *ITA_toolbox* is an open source project developed by the *Institut für Technische Akustik* (ITA), RWTH Aachen University for MatLab by MathWorks©. More information at: <http://www.ita-toolbox.org/>.

3. Theoretical background

In this chapter, basic knowledge about the measurement methods is introduced. Starting with fundamental laws and definitions, and concepts about room acoustics, it continues with a short explanation of listening test and room acoustic simulations.

Despite the knowledge that the reader is assumed in this work, these notes serve as clarifications. To get a deeper view in any of the points, the reader can address the literature mentioned in the bibliography. Basic and previous concepts about the sound propagation models, room acoustic simulations are described in Frank Dierkes' diploma thesis [22].

The theoretical sections are orientated roughly on Brüel's *Sound insulation and room acoustics*.

3.1. Definitions³

Scattering coefficient [S_θ]: Value calculated by one minus the ratio of the specularly reflected acoustic energy to the total reflected acoustic energy.

Random-incidence scattering coefficient [S]: Value calculated by one minus the ratio of the specularly reflected acoustic energy to the total acoustic energy reflected from a surface in a diffuse sound field.

Random-incidence absorption coefficient [α_s]: Value calculated by one minus the ratio of the total reflected acoustic energy to the incident acoustic energy, on a surface in a diffuse sound field.

Random-incidence specular absorption coefficient [α_{spec}]: Value calculated by one minus the ratio of the specularly reflected acoustic energy to the incident acoustic energy, on a surface in a diffuse sound field.

Impedance [23]:

Assuming that for materials dealing with perpendicular incidence it is possible to measure its absorption coefficient by means of the Tube method⁴. According to the previous assumption, the true impedance of an absorbent material is defined as the real, specific impedance greater than that of air, which according to the equation below has an absorption coefficient of α :

$$\alpha = 1 - |R|^2 = 1 - \frac{B^2}{A^2} = \frac{A^2 - B^2}{A^2} = \frac{4}{n + \frac{1}{n} + 2} \quad (1),$$

³ Definitions below given as in the ISO 17497-1, see entry [17] in the bibliography.

⁴ TUMA: Sitzung der Kaiserlichen Akademie der Wissenschaften, III, 2A, p.302, 1902; E. T. Paris: The stationary wave method...; DAVIS AND EVANS: Measurement of absorption power...; W. M. Hall: An acoustic transmission...; P. O. PEDERSEN; Lydtekniske Undersøgelser...; V. L. JORDAN: Electroakustiske Undersøgelser...; P. V. Brüe: Rørmethodens Anvendelse...

where \mathbf{R} stands for reflection factor, \mathbf{n} stands for ratio between optimum and minimum sound pressure $n = \frac{A+B}{A-B} = \frac{P_{\max}}{P_{\min}}$, \mathbf{B} stands for amplitude of the reflected wave and \mathbf{A} for amplitude on the incident wave. But for the absorption coefficient at oblique incidence the relation between the absorption coefficient and the angle of incidence of the sound is:

$$N_{\Theta} = \frac{p}{v} = \frac{p \cdot \cos \Theta}{u} = N \cdot \cos \Theta = \rho \cdot c \cdot \cos \Theta \quad (2),$$

assuming $u = v \cdot \cos \Theta$. As a result, absorption coefficient for oblique incidence stands for:

$$\alpha_{\Theta} = \frac{4}{n \cdot \cos \Theta + \frac{1}{n \cdot \cos \Theta} + 2} = 1 - \left(\frac{n \cdot \cos \Theta - 1}{n \cdot \cos \Theta + 1} \right)^2 \quad (3).$$

3.2. Measuring methods

One of the most relevant acoustic properties is the sound absorption coefficient, dependent on the frequency and angle of incidence. To be able to predict and control acoustics in built environments, measuring absorption characteristics of materials is an important step [24]. According to a crude simplification, geometrical acoustics methods assume that the absorption coefficients of room surfaces are independent of the angle [25]. At the moment of carrying out measurement techniques there is a distinction to make between the different measurement methods and the synthesis methods, which extrapolate data from just one measurement. Methods to produced data can be divided in three different groups: analytical, empirical and *in-situ* methods. In the following paragraphs every group is explained and, in each, different proposals are given.

In-situ methods mostly measure the acoustic impedance by applying two-microphone techniques. The proposed techniques are based on the measurement of the transfer function between two microphones using a spectrum analyzer. The absorption coefficient of absorbing materials can be measured with the impedance tube for normal sound incidence or the Tamura method for normal and oblique incidence of sound [26]. Tamura explained a two-dimensional Fourier transformation is used to calculate the angle dependent surface impedance. Meanwhile *in-situ* methods calculate the corresponding absorption coefficient from the impedance of the surface. Conventional methods such as standing wave tubes test rely on the plane wave assumption and are sensitive to the mounting of the sample [27].

Cox, in another way, explored the possibility of altering sound waves from devices that are constructed just for this measure. The main feature of the construction was made of multiple thin perforated sheets which were spaced half a wavelength apart depending on the frequency, creating the necessary impedance discontinuities to create backscattered waves, which interfere at certain frequencies to create a strong reflected sound. One of the facts he observed was that as the angle of observation changes, the

frequencies at which strong reflections occur alters. While some frequencies of strong reflection increase as the angle of observation gets larger, others decrease [28].

In a different category as those explained, C. -H. Jeong divides the models between empirical models and analytical models. Delany and Bazley, Miki, Mechel and Komatsu model [29] [30] [6] [2] are categorized as empirical models. On the other hand, Beranek's model [31] is a fully analytical model. At the same time, analytical wave propagation models are classified in two groups: rigid-frame and elastic frame models. The wave propagation models require several parameters in order to explain the behavior of sound in a mixed structure of fluid in solid frame [25].

However, not all methods described are measurement methods. Komatsu sum up all the previous works, improving them, of what we could say synthesis methods: from just one data and measurement could extrapolate the rest of the data for angle-dependent absorption coefficient. Komatsu showed a new form for predicting the acoustical properties of fibrous materials, taking as starting point the Delany-Bazley and Miki models. Both Delany-Bazley and Miki models are applied to porous materials, but the expressions to calculate the properties of porous sound-absorbing materials could only be deduced from their airflow resistivity. When it comes to predict high-density fibrous materials, this new model is more effective than conventional models. Based on the two-cavity method according to the transfer-function method of ISO 10534-2 and airflow method specified in ISO 9053. It is clear that Delany-Bazley and Miki models increase the error of sound absorption coefficient, as well as, prediction errors of the characteristic impedance and propagation constant. With the Komatsu model these errors are reduced to small values [2].

Knowing the absorption coefficient is important for several applications. In room acoustics characteristics can be predicted, if there is knowledge of the behavior of materials.

3.3. Angle-dependent absorption coefficient

The absorption coefficient, in cases, depends on the angle of sound incidence. However, an angular average of the absorption coefficient derived using the Paris' formula can be used to estimate a random-incidence value [32]. The method described by Mommertz [14] is mainly intended for experimentally checking the absorption coefficient *in-situ*, for example, of wall surfaces in rooms. So the Paris' formula is presented as:

$$\alpha_{ran}(f) = \int_0^{\pi/2} \alpha(f, \Theta) \cdot \sin(2\Theta) \cdot d\Theta \quad (4).$$

The subtraction technique allows accurate and fast measurements of the frequency and angle-dependent reflection coefficient in combination with the use of pseudo noise signals with equalizing properties, which improves the reflection method and enables the frequency dependent coefficients to be determined at almost arbitrary angles.

The method is basically intended to measure the absorption coefficients of the wall surface *in-situ*, to estimate the random sound absorption coefficients, measurements can be made at different angles of incidence and random incidence values are estimated by Paris' formula.

Although interference phenomena are an important issue to be considered in room acoustics, computer models treat sound reflections more as carriers of sound energy [33]. Therefore, reflections are treated as pressure waves, –with amplitude–, to calculate the sound pressure impedances of surfaces.

The statistical absorption coefficient, α_s is approximated by an angle of incidence $\theta = 60^\circ$ under diffuse field conditions. According to this assumption, the pressure reflection factor can be estimated by:

$$r_{60} \approx \pm\sqrt{1-\alpha_s} \quad (5)$$

where r_{60} can be either positive or negative. From (6) equivalent real impedance of the reflecting surface can be calculated as:

$$Z_a = Z_f^* \frac{1+r_{60}}{1-r_{60}} \quad (6)$$

here Z_f^* stands for the equivalent field impedance of the test sample as measured under diffuse field conditions. With the results obtained in the previous two equations the general expression for the pressure reflection factor can be determined by the equation:

$$r_\theta = \frac{Z_a - Z_f(\theta)}{Z_a + Z_f(\theta)} \quad (7).$$

3.4. Non-locally reacting materials

A surface is termed non-locally reacting, when the surface impedance is dependent on the nature of the incident wave. Besides, the reaction of the material at any point is dependent on the reaction at other points⁵.

Porous materials are considered as locally reacting for waves in a plane perpendicular to the channels, but it is not for any other angle. Otherwise, the absorber is purely non-locally reacting in a plane parallel with the channels [34].

So far, as Hopkins states, “it has been assumed that although the sound waves impinging upon a surface are absorbed, this absorption is a ‘local matter’ between the points on the surface from which is reflected. Assumption of locally reacting room surfaces is very useful in simplifying the calculations of the reverberation time. Many absorbers, such as porous absorbers, or small areas of rigid frame can be considered as locally reacting” [35].

⁵ This definition is provided by the author after a modification of the locally reacting materials explanation given by T. J. Cox and P. D’Antonio [5].

It can also be assumed that the acoustic sample is locally reacting, when it has a large refraction index. This consideration simplifies the equations that govern the sound field above the sample, allowing the assessment of the surface impedance and the corresponding absorption coefficient through a relatively simple iterative algorithm [36].

Considering the surface as locally reacting is another extremely useful first order approximation. As Cox and D'Antonio explain, "it means that in multi-layered absorbers the propagation can be assumed normal to the surface and are therefore much easier to evaluate". However, when non-linear propagation is significant due to large sound pressure differences, these assumptions will break down [5].

3.5. Room acoustics simulation

The ray tracing and image source method are two classical geometrical methods for the simulation of sound in rooms. Ray tracing models create high order reflections, using, also, a large number of particles emitted in various directions from a source point. Meanwhile the image source model is based on the principle that a specular reflection can be constructed geometrically by mirroring the source.

3.5.1. Image source model

The image source model is a geometrical approach to the point-to-point transfer function of a room [37]. This approach uses image sources, which are defined by treating every boundary as mirrors in which the actual source can be reflected. The distance of the propagation path from source to receiver is equal to the length of straight line from image source to the receiver.

3.5.2. Stochastic ray tracing

An alternative approach, in contrast of the image source model, is the stochastic ray tracing algorithm [38]. Capable of using the scattering and diffusion coefficients too, a large number of particles are emitted by the sound source, each carry a certain amount of energy. Initially, the energy and direction of the particles are distributed uniformly, not depending on the directivity of the source. The receiver, commonly represented as a sphere, is a volume detector. Thus, the energetic envelope of the room impulse response (RIR) shows the travel of each particle through the volume, time and current energy of the particle.

3.5.3. Auralization

Auralization is the technique of creating and reproducing sound on the basis of computer data, as described by M. Vorländer [39]; allowing the prediction of the behaviour of sound signals. These signals are generated by a source and modified by reinforcement, propagation and transmission in different systems, such as rooms or buildings.

The main aim of auralization is to create an aural impression of a source playing inside a room [40]. To create the aural impression of the simulated hall,

the headphones method, which provides a binaural room impulse response (BRIR), is used by listeners. The acoustics properties of a room for a specific sources-microphone configuration can be completely represented using the impulse responses.

3.6. Listening test

A listening test is a test where one or more persons in a systematic way are presented with samples of sound and requested to give their evaluations/response in a prescribed manner. A listening test can be either objective or subjective [41]. There are two basic considerations that govern the use of any experimental procedure: (1) the placing of observations and (2) estimation based on the resulting data [42].

At the time to perform a listening test, there are some common criterions to be considered among the wide range of types which can be chosen. First of all, before running the listening test, a target must be defined, according to the goal of the study. Therefore, as the aim gives a starting point, characteristics of the listening test can be defined, such as: what is the question proposed to the subject, which answer the individuals must give or if the test must resemble a real-life experience.

The test for the purpose of this thesis is a three-alternative forced-choice. One of the main reasons to use this test is that the subject is forced to give an answer. So, no iteration is left without an answer. An important assumption must be considered when the listening test is carried out: subjects, in some cases, tend to avoid a decision, so random answers should be estimated in advance. Therefore, it is important to assure inexperienced subjects that there are no wrong answers in a listening test [43]. Furthermore, while there is generally no time pressure or reward for speed, it is likely that the subject attempts to reach a final adjustment in a minimum amount of time [44]. Besides, an assumption for the time between samples that the human hearing system is capable of remembering a sound level in the short-term memory, for instances: for stationary signals, normally a length between 3 and 5 seconds is sufficient.

Before the listening test takes place, a sheet with instructions is given to the individual. If inconsistent trials occur with various subjects, this could indicate that individuals did not understand the task correctly or subjects may be overtaxed. Moreover, the evaluators must take recognition of the audio capacity of the person taking the exam, to assure there are no hearing problems. Listening tests must take place in an adequate environment. The evaluation of the test shows the perception of the changes by the listeners.

3.6.1. Test setup: three-alternative forced-choice

The three-alternative forced-choice is a standard psychoacoustic procedure. For the case of forced-choice experiments, a positive response may be defined as identifying the correct or wrong observation. The proportion of positive responses, with equal stimuli, corresponds to random guessing and is determined by the number of possible alternatives [42]. In our case 33% is referred to our lower border for the evaluation rate. This case allows greater accuracy compared to other listening tests used, locating the

random response level by the user in a lower percentage. For instance, a two choice listening test where the subject knows there is a difference between A and B and the right answer chance is set to a 50%, even when answers are given in a randomly way. However, carrying out a forced-choice test with more than 3 stimuli is not suitable, although lower boundary increases accuracy; because the subject will not remember the signals after the first audition and will have to repeat them several times until getting an idea, making the test last for too long. Due to this time period, the individual can get tired, provoking a probably inconsistent answer.

Three sound samples are presented to the subject in succession. The listeners are asked to judge these three sounds according to a certain criterion. Regardless to other forced-choice experiments, in this case there is no positive or negative response defined, such as identifying the correct observation interval [42]. Listeners are instructed to indicate the “odd-one-out” without receiving trial by trial feedback. Results are stored and analysed later.

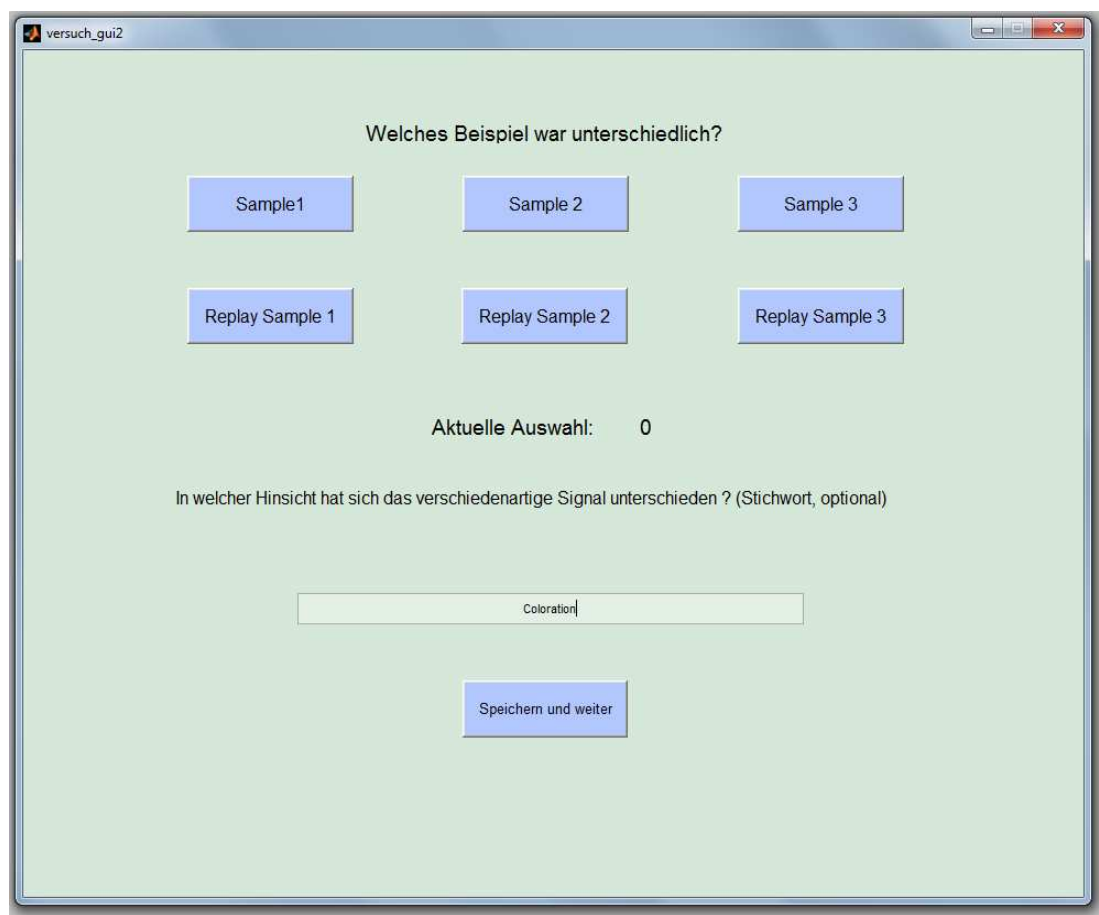


Figure 1: Screenshot of the interface used in the listening test by subjects. There are three buttons to replay the sample, when needed, and a text field where any comment could be given.

4. Application of angle-dependent absorption coefficient in room acoustics simulations

As described in sections 3.4 and 3.6, room simulation and a listening test were run to evaluate the perception of angle-dependent absorption coefficients. This chapter will discuss the work done to obtain the results and explain the functioning of the process. The computer simulation relies on a hybrid simulation, as the *RAVEN* simulation software combines both image sources and ray tracing. The binaural room impulse response was synthesized by using head-related transfer functions (HRTF). The *Matlab* implementation is described in the next section, as well as, the following steps.

The listening test was based on a three-alternative forced-choice option, as explained in the previous section. After convolving the simulated room impulse response with the different signals, individuals were required to proceed to the subjective evaluation.

4.1. Example rooms and example materials

To analyse the influence of angle-dependent absorption coefficients, different rooms were modelled. As the non-uniformity over the angle of incident energy was higher in the box-shaped room than in the other rooms considered, the model was chosen for the analysis. So to carry out first simulations a box-shaped room, close to a lecture hall, was used. The size of the room is 15x7x4 meters (Figure 2). The energy distribution was analysed over the angle of incidence, still assuming diffuse sound reflections of surfaces in the room.

For the simulation, the walls were covered with different materials. The smallest rear wall was covered with the materials designed by the author, one at the time, as explained below. The other five walls were covered with materials with varying scattering and absorption coefficients ($0\% \leq S \leq 20\%$ and $0 \leq \alpha \leq 1$). Hence obtaining eighteen different cases to introduce either of each two signals, a pink noise burst or a natural signal containing a piano melody (Chopin's piano concert sample), and study the effects. Pink noise contains all frequencies and the energy in all octaves is the same. The human hearing system does not perceive frequency octaves with equal sensitivity, because the frequency processing in the ear is a roughly logarithmic approximation. Pink noise is targeted to match the frequencies of human speech raised the threshold of audibility just enough to mask intelligibility without requiring a higher loudness, as used in earlier systems. This broadband and transient signal proved in pretests and former studies to be very sensitive and enabling high detection rates. The second signal was a natural signal containing a piano melody. Selection was made because it also covers a wide frequency range and includes percussive chords as well as a fast melody. It is, also, an updated approximation of music's typical spectrum.

4. Application of angle-dependent absorption coefficient in room acoustics simulations

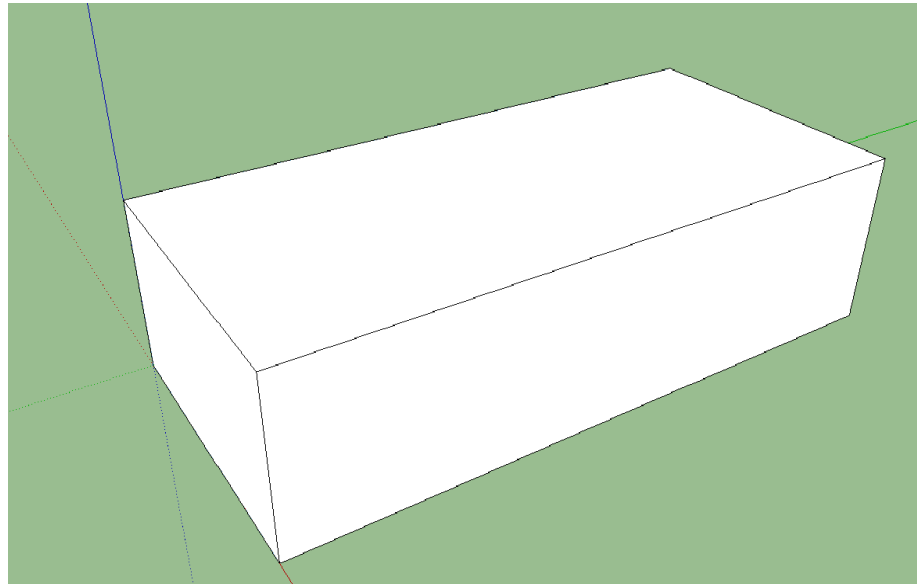


Figure 2: Box-shaped room. Screen capture from the Sketch up model used as the example room, which size is 15x7x4. The absorber wall was placed in the small wall (7x4) seen on the left side of the picture.

The room volume of 620 m³ is a typical size for a lecture hall or a small concert place. The absorber was located over the rear wall of the scenario. Other rooms designed for further simulations in this thesis were: a long corridor, an L-shaped corridor and a multiform building.

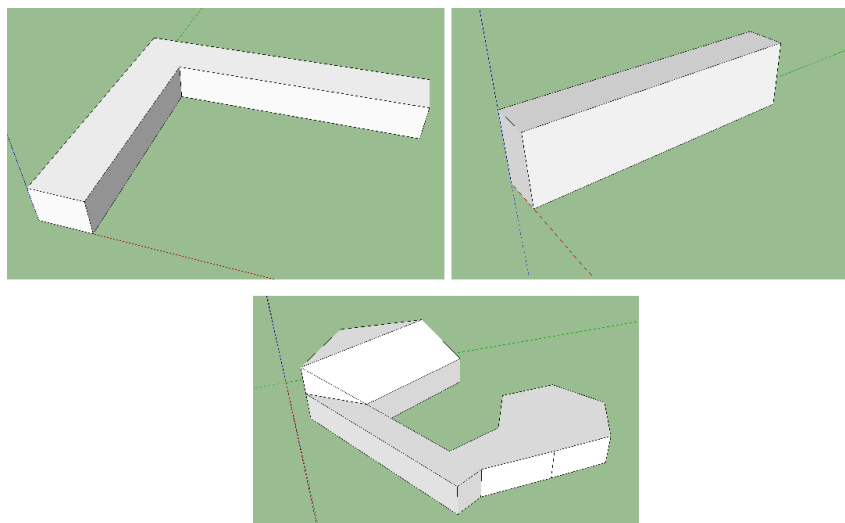


Figure 3: Alternative example rooms for future simulations.

To get the highest impact in the results, three layered materials, which would have an unnaturally high non-uniformity of the angular reflection factors over the full broadband frequency range, were designed. All of them were created by the author, so any resemblance to a real material would be a coincidence. The reason to choose these invented materials is based on the idea of getting extreme cases to actually perceive the changes. When it comes to design the characteristics, the *ita_impcalc_gui* function was used. Between the materials used to the configuration, the user can choose: basalt-wool,

perforated plate, absorber material based on the Komatsu model. Also, in the characteristics size, surface or, in the case of the last example, the airflow resistivity, which was introduced using Figure 17 and Figure 18, enclose in Appendix A, [45] [46]. All was then stored in the database generated by the **Matlab** function.

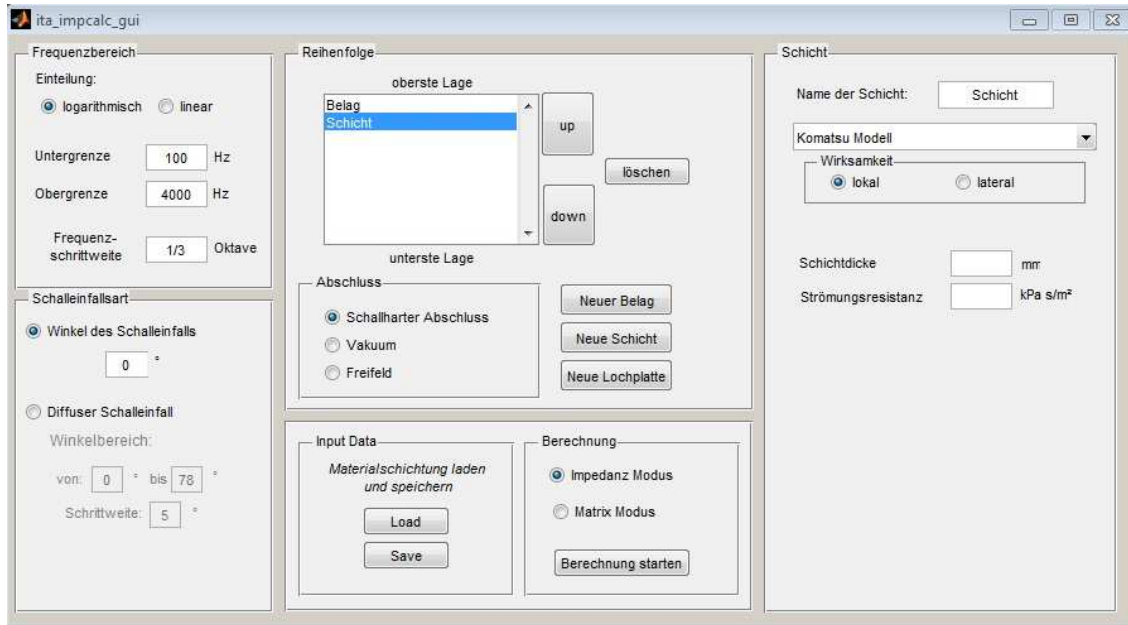


Figure 4: *ita_impcalc_gui* interface. The screenshot shows the different options at the time the user wants to create a new material with different layers.

The materials created are: (1) Basalt wool-Air-Perforated plate-Air-Wall, (2) Perforated plate-Air-Basalt wool-Wall, (3) Porous material-Air-Basalt wool-Thick air-Perforated plate-Thin air-Wall, as seen in Fig. 5. The following figures (Fig. 6, Fig. 7 and Fig.8) represent the polar diagrams of each material. For the diagrams interpretation the reader should know that: the outer part of circumference shows the angle of incidence, from 0° to 180° . And the different coloured lines inside represent the frequencies (given in the legend of each diagram) and absorption coefficient for each one by the radius. The model in the simulation was run from 0° to 90° and from that end to 180° , a mirror drawing was applied considering the symmetry produced in the material behavior. To implement that the angle increase changes automatically the property *saveIt.sea.winkle* in the *ita_impcalc_gui* change in an interval of 5° (*saveIt.sea.step*), covering an interval of angles from 0° to 90° .

4. Application of angle-dependent absorption coefficient in room acoustics simulations

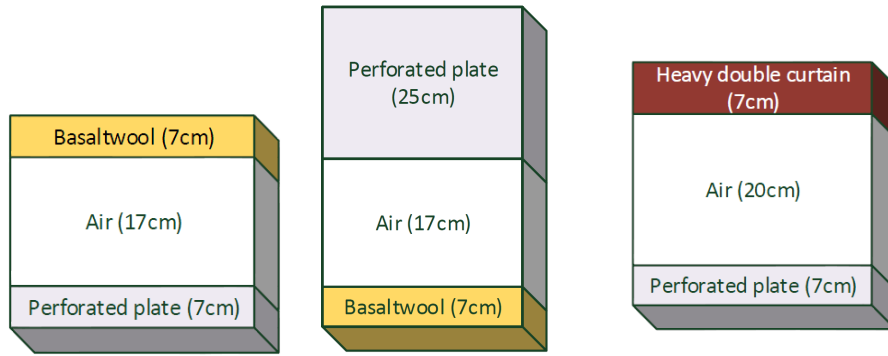


Figure 5: Sketch of the layered materials. In order: Material 1, Material 2 and Material 3 explained in the previous paragraph.

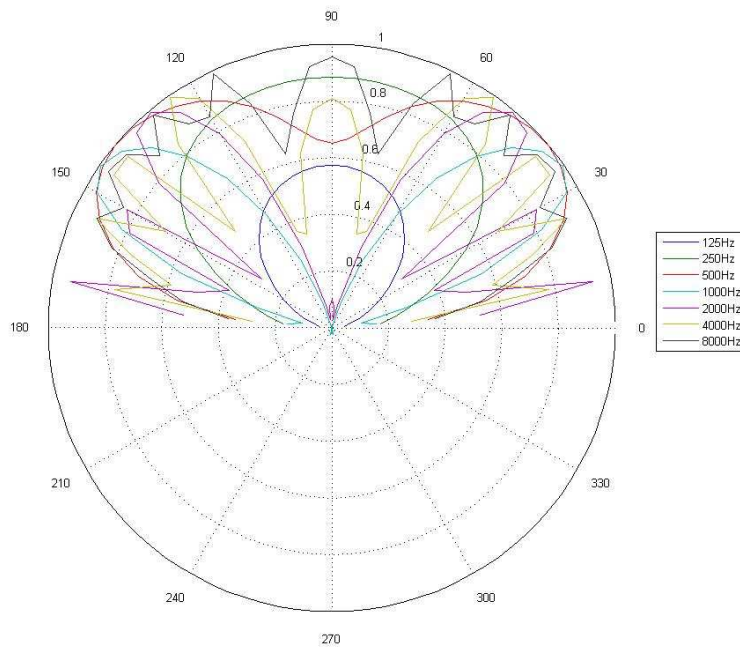


Figure 6: Polar diagram corresponding to the second material composed of Basalt wool-Air-Perforated plate (Material 1).

4.1. Example rooms and example materials

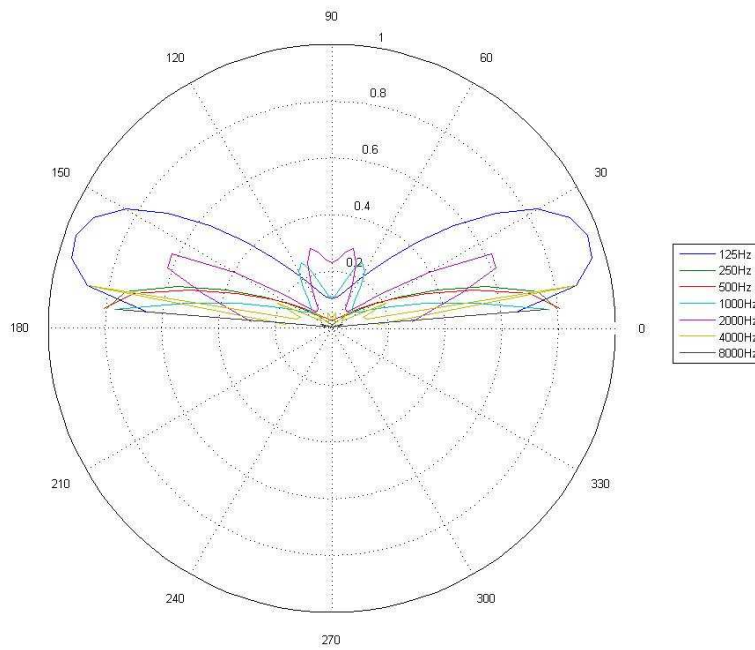


Figure 7: Polar diagram corresponding to the second material composed of Perforated plate-Air-Basalt wool (Material 2).

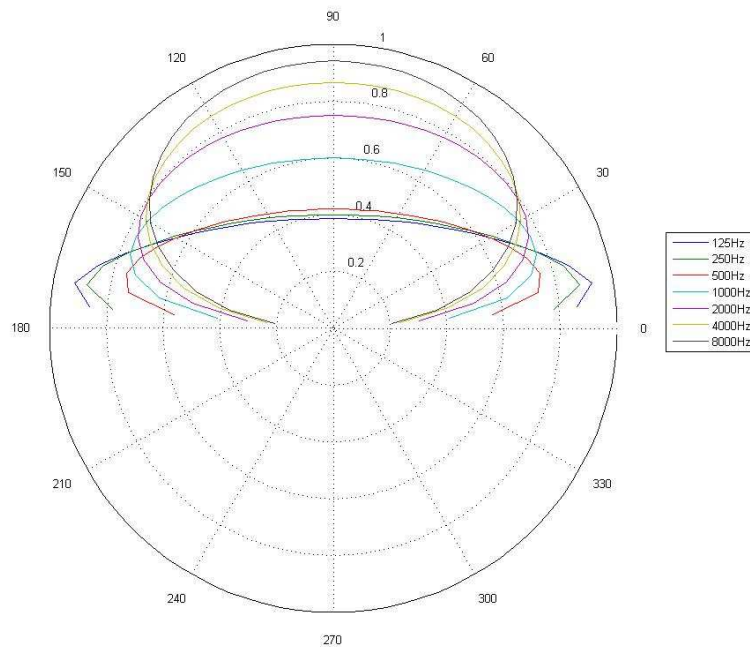


Figure 8: Polar diagram corresponding to the second material composed of Porous material-Air-Basalt wool-Thick air-Perforated plate-Thin air (Material 3).

4.2. Binaural room impulse response simulation, RAVEN and auralization

To obtain the result for each angle corresponding to the incident sound wave in the simulation, the following process was carried out.

First step was opening the signal later used for the listening and save it as a variable. In this case is shown the pink noise burst.

```
uiopen('C:\Program
Files\RAVEN\RavenDatabase\SoundDatabase\Pinknoise_Bursts.wav',1);

sound_signal = Pinknoise_Bursts;
```

The rooms modeled with Google SketchUP and export as a **RAVEN** project (*.rpf) are now import to set the characteristics of the simulation. There are two cases for each material: angle-dependent absorption coefficient, named the variable as '*rpf*', and the diffused coefficient material, differenced with a '*_d*' always in the names regarding to it.

```
rpf = RavenProject('...\RavenInput\2faces\ShoeBox2fad1case2.rpf');
rpf_d =
RavenProject('...\RavenInput\2faces\ShoeBox2diff1case2.rpf');
```

Setting the order of image sources for the BRIR.

```
rpf.setISOrder_PS(4);
rpf_d.setISOrder_PS(4);
```

As the model is implemented with the stochastic ray tracing method, the use of a higher number of particles increases the accuracy in the results.

```
rpf.setNumParticles(100000);
```

After setting the parameters, the room acoustics simulation was run.

```
rpf.run
```

The binaural room impulse response was obtained. Later it was convolved with the sound signal loaded in the beginning.

```
ir = rpf.getBinauralImpulseResponseItaAudio();
ir_d = rpf_d.getBinauralImpulseResponseItaAudio();

erg = ita_convolve(sound_signal,ir);
erg_d = ita_convolve(sound_signal,ir_d);
```

After running the simulation, a file with the corresponding auralization of the signal in the room was obtained. This audio file was later used for the listening test.

4.3. Analyzed room acoustics parameters

To compare the different acoustic parameters and the behavior of the signal, four characteristics are calculated after the process described in 4.1. The Reverberation Time ($T_{30}/T30$), the Clarity ($C_{50}/C50$), the Early Decay Time (EDT) and Strength (G).

Results, given in different charts, showed the average data variation for each frequency and angle of incidence, due to the configuration of the room.

```
T30 = rpf.getT30;
T30_d = rpf_d.getT30;

Clarity = rpf.getClarity;
Clarity_d = rpf_d.getClarity;

EDT = rpf.getEDT;
EDT_d = rpf_d.getEDT;
```

The x-axis was defined regarding to the central frequencies corresponding to an octave resolution.

```
x = [31.5 63 125 250 500 1000 2000 4000 8000 16000];
```

All data was stored in a vector and later represented in charts.

```
T30 = [(T30_11)';
(T30_12)';(T30_13)';(T30_21)';(T30_22)';(T30_23)';(T30_31)';(T30_3
2)';(T30_33)'];

[...]

C50 = [C50_11;
C50_12;C50_13;C50_21;C50_22;C50_23;C50_31;C50_32;C50_33];

[...]

EDT = [(EDT_11)';
(EDT_12)';(EDT_13)';(EDT_21)';(EDT_22)';(EDT_23)';(EDT_31)';(EDT_3
2)';(EDT_33)'];

[...]
```

Figures 9 and 10 in the next chapter show the final data.

4.4. Conducting the listening test

For the listening test, the lecture hall model was simulated with the materials described in section 3.4.4, each with diffused coefficient and angle-dependent reflection modeling. A 32 question test was generated. Answers were evaluated as right or wrong, although the goal was to judge the listeners capacity to perceive the changes. Source signals were presented at listening levels between 78 and 84 dB(A). The first was a sequence of three pink noise burst, each with 120 ms duration and 210 ms pause. The second signal was chosen to be a natural signal and contained a piano recording of 3.8 s length.

Before taking the questionnaire, blocks of questions were randomized in order. For each trial, the mix is different, so subjects do not repeat the same test, avoiding a bias by learning effects. Blocks are shuffled, remembering the initial order (at the end of the explanation the code is showed). Results, after running the test, are reordered in the initial position and saved as a Microsoft Excel file.

4. Application of angle-dependent absorption coefficient in room acoustics simulations

At the moment of conducting the listening test, the following instructions, in a written form, were given to the subjects: (1) 3 signals input will be played, one after the other. There will be a little pause between them, so the subject will distinguish the signals, but will not forget them. (2) Two of the signals are the same and the other one is different. Example: The listener will hear signal A, signal A and signal B. (3) After hearing the three signals the subject should give an answer clicking the button of the signal which he thinks is different. (4) If you missed one signal due to any disturbance, each signal can be repeated.

23 subjects, all trained experts with experience in listening tests, participated in the experiment. In this case, all of them were members of the staff of the *Institut für Technische Akustik* (ITA), which makes all of them have a theoretical background in Acoustics. No previous laboratory trial was allowed, so the individuals took the listening test just after reading the instructions.

The following code, introduced in the *ita_listeningtest_3afc_prueba.m*, shuffle the blocks each time the test takes place:

```
% SUFFLE DATA BLOCKS AND SORT ANSWER AFTER TEST %
% Author: David Vázquez Rufino
% 2013
clc
clear all

%% INPUT DATA
blocklength= 2;
repeat=1;
%Read files
[files] = textread('survey.txt','%s');
num_files = length(files);
num_pairs = length(files);
%Build block
block_length=num_files/blocklength;
block=cell(block_length,2);
for k=1:block_length
    block(k,1)=files(2*k-1);
    block(k,2)=files(2*k);
end

%% SUFFLE BLOCK
suffle=randperm(block_length);
newblock=cell(block_length,2);
for i=1:block_length
    newblock(i,:)=block(suffle(i),:);
end

%% TEST RESULT
% Answer corresponds: 1=yes, 0=no, 2=don't know
% testresult is a (1 x block_length) vector with the answer
codified
% this is a random example, real answer vector must be here
testresult=round(rand(1,block_length));
```

```
%% SORT ANSWER
sortanswer=zeros(size(testresult));
for l=1:block_length
    position=find(suffle==l);
    sortanswer(l)=testresult(position);
end
```


5. Discussion of results

Objective results, obtained after running the simulations, show the average data obtained to understand the behaviour of the different materials according to the reflection modeling applied in the case studied. The data analysis in this part of the thesis is the different room acoustics parameters, such as reverberation time. All these characteristics depend strongly on the absorption coefficients of the different materials which cover the surfaces of the room.

5.1. Room acoustic parameters results

The analysis of the angles of incident energy showed that in the scenario of the box-shaped room, the non-uniformity was high. This was the main reason to choose this room. The results show that there is a variation depending on the type of reflection modeling. All three materials presented were applied to the rear wall, once using angle-dependent reflection and once using diffuse-average values. Other parameter variations addressed the mean absorption and scattering coefficients of the remaining walls. The different cases were calculated: (a) considering two different scattering values, 0 and 0.2; and (b) changing the absorption coefficient of the 5 surfaces between $\alpha = 0.02$; 0.2 and 1 for the computer simulation test. For the listening test convolved audio file these parameters were changed to $\alpha = 0.15$ and $\alpha = 0.3$. For $\alpha = 1$, no reverberation time values are given in Figures 9 and 10, because the room is semi-anechoic then.

For every frequency an average value is given, according to a 5° incidence angle variation. As predicted, before running the simulations, from the polar diagrams (Figures 6, 7 and 8), results in the tables are as expected: the influence of the materials of the remaining walls conditions the decrease in the values of the T_{30} , C_{50} and EDT. But the absorption behavior shown in the polar diagrams is reflected in the average data obtained below.

Case 1 $\alpha = 0,02$						
T30 / Material	angle dependent 1	angle dependent 2	angle dependent 3	diffuse material 1	diffuse material 2	diffuse material 3
T30 _{31,5Hz}	7.4356	7.3148	7.6500	10.1618	5.2240	8.9488
T30 _{63Hz}	7.2002	8.3448	8.2544	10.0989	10.4492	9.4011
T30 _{125Hz}	7.5589	8.2921	8.1289	9.6382	10.3249	9.1649
T30 _{250Hz}	7.8396	7.8838	7.4735	9.1905	7.7417	9.2104
T30 _{500Hz}	8.2156	5.3807	7.5313	8.7921	7.0926	8.5264
T30 _{1KHz}	7.0637	4.4369	6.8558	7.6268	6.3492	7.5643
T30 _{2KHz}	5.4924	5.2594	5.5201	5.8132	5.0554	5.7734
T30 _{4KHz}	3.1258	3.0687	3.1492	3.1839	2.2987	3.1709
T30 _{8KHz}	1.2221	1.1231	1.2251	1.2206	0.9807	1.2274
T30 _{16KHz}	0.4224	0.4365	0.4220	0.4215	0.4516	0.4248

Table 1: Average results of T_{30} changing the rear wall applying the angle-dependent reflection and diffuse-average values of the three materials used for the simulation. The scattering value is constantly ($\alpha = 0.02$).

5. Discussion of results

Case 1 $\alpha = 0,02$						
Clarity 50 / Material	angle dependent 1	angle dependent 2	angle dependent 3	diffuse material 1	diffuse material 2	diffuse material 3
Clarity _{31,5Hz}	-3.3738	-8.7028	-6.4780	-2.9363	-7.0817	-3.7906
Clarity _{63Hz}	-2.9386	-4.8331	-4.5535	-3.5835	-3.3139	-2.7557
Clarity _{125Hz}	-3.1573	-4.1981	-3.6512	-3.9857	-4.9256	-2.8789
Clarity _{250Hz}	-3.8419	-7.4951	-3.3627	-4.6136	-4.2064	-3.1763
Clarity _{500Hz}	-4.8542	-6.5941	-3.5415	-5.7017	-3.2311	-4.0200
Clarity _{1KHz}	-5.2276	-5.5277	-4.0235	-5.8045	-3.2310	-4.8154
Clarity _{2KHz}	-4.8883	-3.7219	-4.2665	-5.3020	-2.3495	-4.7887
Clarity _{4KHz}	-3.3903	-2.6889	-3.1780	-3.4968	-2.1403	-3.3975
Clarity _{8KHz}	0.4573	0.1404	0.4551	0.4121	1.1814	0.4905
Clarity _{16KHz}	8.2668	7.4284	8.3428	8.2610	7.0930	8.1429

Table 2: Average results of C_{50} changing the rear wall applying the angle-dependent reflection and diffuse-average values of the three materials used for the simulation. The scattering value is $\alpha = 0.02$.

Case 1 $\alpha = 0,02$						
EDT / Material	angle dependent 1	angle dependent 2	angle dependent 3	diffuse material 1	diffuse material 2	diffuse material 3
EDT _{31,5Hz}	2.7035	6.2499	4.4467	4.5252	4.3657	2.5759
EDT _{63Hz}	2.9829	3.9898	3.1352	5.0430	4.7752	3.3676
EDT _{125Hz}	3.4318	3.8507	2.8900	5.2305	5.4842	4.0984
EDT _{250Hz}	4.2251	5.9767	3.1329	5.3151	2.6301	4.4541
EDT _{500Hz}	4.5243	4.3980	3.6507	5.1572	2.3888	4.6864
EDT _{1KHz}	4.3577	3.2394	4.0487	4.8153	2.2967	4.5262
EDT _{2KHz}	3.7596	3.1347	3.6495	3.8968	2.0314	3.8256
EDT _{4KHz}	2.4504	2.0456	2.3991	2.5319	1.6669	2.4336
EDT _{8KHz}	1.1168	1.1150	1.1121	1.1271	0.9688	1.1215
EDT _{16KHz}	0.4399	0.4596	0.4362	0.4407	0.4759	0.4458

Table 3: Average results of EDT changing the rear wall applying the angle-dependent reflection and diffuse-average values of the three materials used for the simulation. The scattering value is $\alpha = 0.02$.

Case 2 $\alpha = 0,2$						
T30 / Material	angle dependent 1	angle dependent 2	angle dependent 3	diffuse material 1	diffuse material 2	diffuse material 3
T30 _{31,5Hz}	1.3096	1.5326	1.4417	1.5825	1.3461	1.2376
T30 _{63Hz}	1.3664	1.5136	1.3153	1.7126	1.6844	1.4980
T30 _{125Hz}	1.4807	1.4416	1.3273	1.7220	1.7447	1.5757
T30 _{250Hz}	1.6356	1.5099	1.3748	1.7286	1.1924	1.6700
T30 _{500Hz}	1.6613	1.3704	1.5152	1.6994	1.2448	1.7040
T30 _{1KHz}	1.6389	1.2209	1.6124	1.6608	1.1511	1.6729
T30 _{2KHz}	1.5618	1.3593	1.5050	1.5791	1.1394	1.5854
T30 _{4KHz}	1.2455	1.0746	1.2425	1.2532	0.9114	1.2553
T30 _{8KHz}	0.7405	0.6481	0.7371	0.7411	0.6026	0.7415
T30 _{16KHz}	0.3284	0.3304	0.3283	0.3293	0.3413	0.3293

Table 4: Average results of T_{30} changing the rear wall applying the angle-dependent reflection and diffuse-average values of the three materials used for the simulation. The scattering value is $\alpha = 0.2$.

Case 2 $\alpha = 0,2$						
Clarity 50 / Material	angle dependent 1	angle dependent 2	angle dependent 3	diffuse material 1	diffuse material 2	diffuse material 3
Clarity _{31,5Hz}	2.1576	-0.1968	0.6385	2.9945	0.2733	1.8308
Clarity _{63Hz}	2.5610	1.5313	1.4750	2.7983	2.9020	2.8113
Clarity _{125Hz}	2.5760	1.6131	2.0359	2.5150	1.6403	3.0088
Clarity _{250Hz}	2.2689	0.2560	2.3543	1.7559	1.4995	2.9002
Clarity _{500Hz}	1.4128	0.4988	2.3854	0.6698	2.1714	2.2444
Clarity _{1KHz}	0.9658	0.8716	1.9781	0.3588	2.0727	1.3819
Clarity _{2KHz}	0.8977	2.1534	1.4596	0.5040	2.6634	0.9354
Clarity _{4KHz}	1.3867	2.4135	1.6235	1.2254	2.6267	1.3620
Clarity _{8KHz}	3.7198	4.1294	3.7839	3.6487	4.8623	3.6858
Clarity _{16KHz}	10.3989	10.2445	10.4158	10.3345	9.8926	10.3356

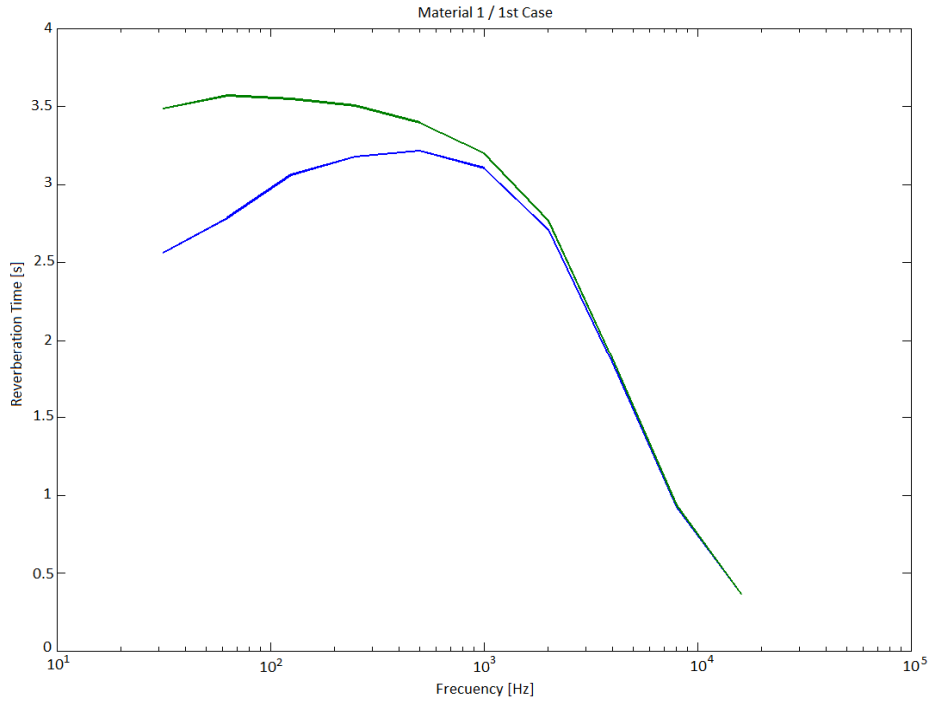
Table 5: Average results of C_{50} changing the rear wall applying the angle-dependent reflection and diffuse-average values of the three materials used for the simulation. The scattering value is $\alpha = 0.2$.

Case 2 $\alpha = 0,2$						
EDT / Material	angle dependent 1	angle dependent 2	angle dependent 3	diffuse material 1	diffuse material 2	diffuse material 3
EDT _{31,5Hz}	0.8210	1.1927	1.0440	0.7325	1.1038	0.8679
EDT _{63Hz}	0.7720	0.9565	0.9311	0.8228	0.7738	0.7395
EDT _{125Hz}	0.7768	0.9725	0.8377	0.9343	1.0351	0.7308
EDT _{250Hz}	0.9112	1.1500	0.8097	1.0204	0.9213	0.7762
EDT _{500Hz}	1.0224	1.0913	0.8263	1.1076	0.8141	0.9714
EDT _{1KHz}	1.0632	0.9951	0.9546	1.1143	0.8241	1.0445
EDT _{2KHz}	1.0470	0.8696	0.9939	1.0769	0.7540	1.0546
EDT _{4KHz}	0.9616	0.7868	0.9439	0.9732	0.7553	0.9685
EDT _{8KHz}	0.6499	0.6301	0.6456	0.6559	0.5799	0.6528
EDT _{16KHz}	0.2629	0.3348	0.2624	0.2971	0.3460	0.2970

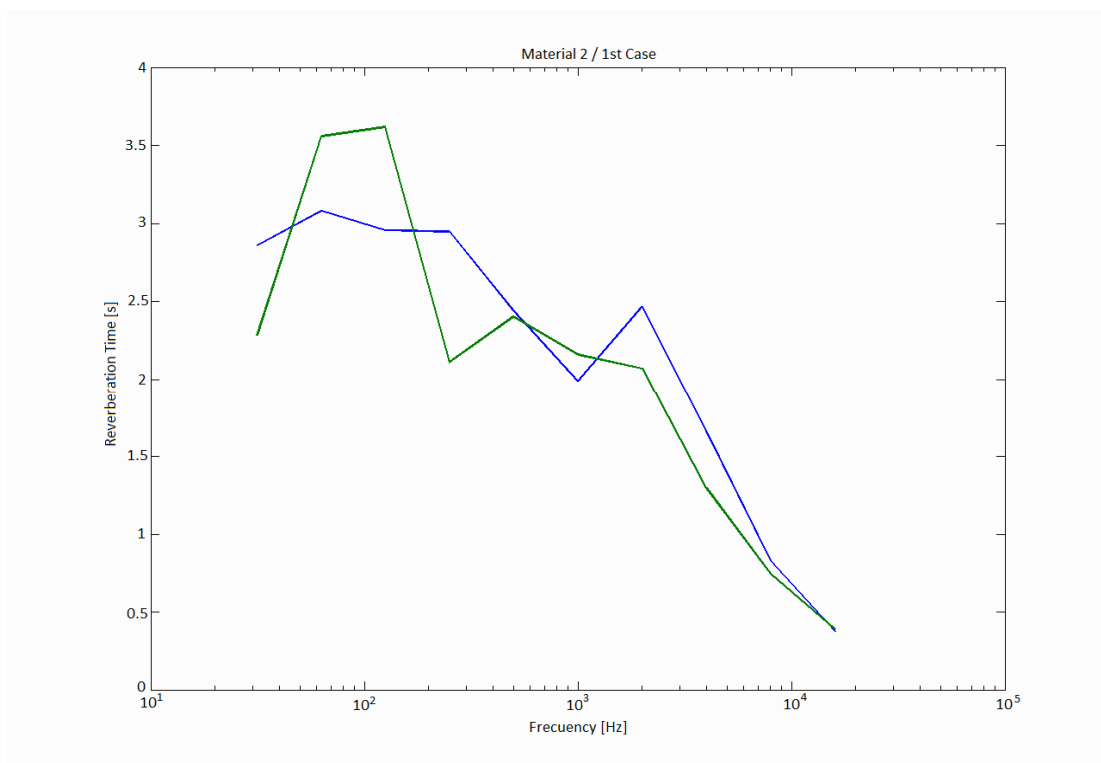
Table 6: Average results of EDT changing the rear wall applying the angle-dependent reflection and diffuse-average values of the three materials used for the simulation. The scattering value is $\alpha = 0.2$.

In comparison, the deviations below show noticeable differences of each parameter. As shown in Figures 9 and 10, the reverberation time difference compared between the diffused average and the angle-dependent are stronger in material B. Highest deviations between diffuse and angle-dependent modeling occurred in cases regarding to material B (Material 2 Cases: 1 and 2. See Figures: 9(b), 9(e), 10(b) and 10(e)), due to the non-uniformity of material B (see Figure 7). In comparison, the deviations of material 1 and 3 were rather small and mostly below the just noticeable differences of each parameter, as shown in Figure 9 and 10. For every case, the differences and changes happened mostly in low and middle frequencies, where the deviation for the reverberation time is over the 10% and for the clarity is over 2 dB, which the definition for each case says is the minimum value to appreciate a change.

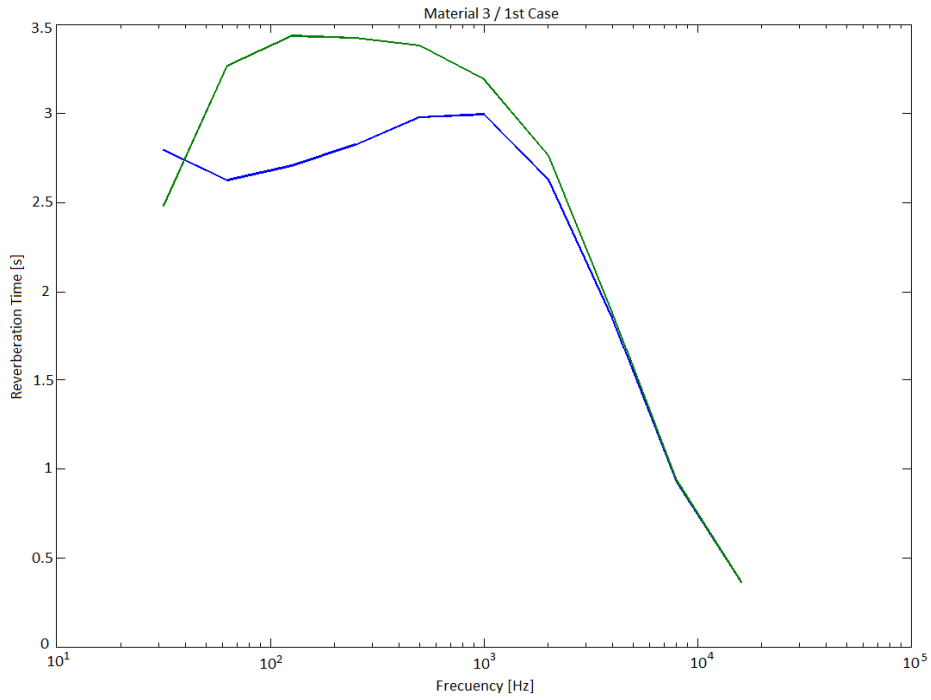
5. Discussion of results



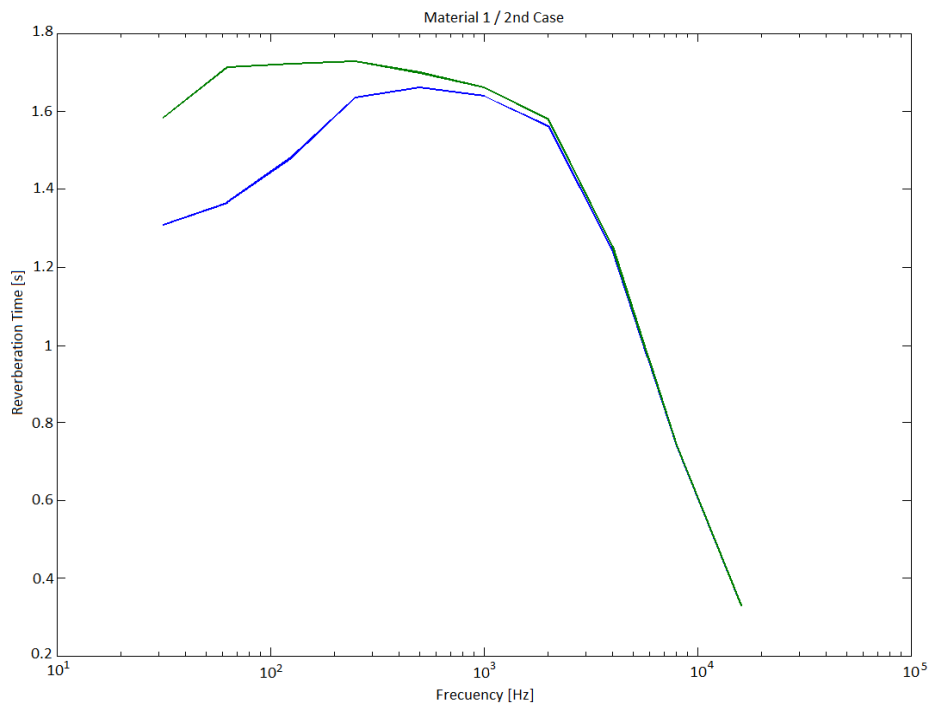
9 (a): Results for the reverberation time for the case one with $\alpha = 0.02$ and zero scattering. The graphic shows the angle-dependent (blue line) and diffused averaged (green line) modeling for material 1.



9 (b): Results for the reverberation time for the case one with $\alpha = 0.02$ and zero scattering. The graphic shows the angle-dependent (blue line) and diffused averaged (green line) modeling for material

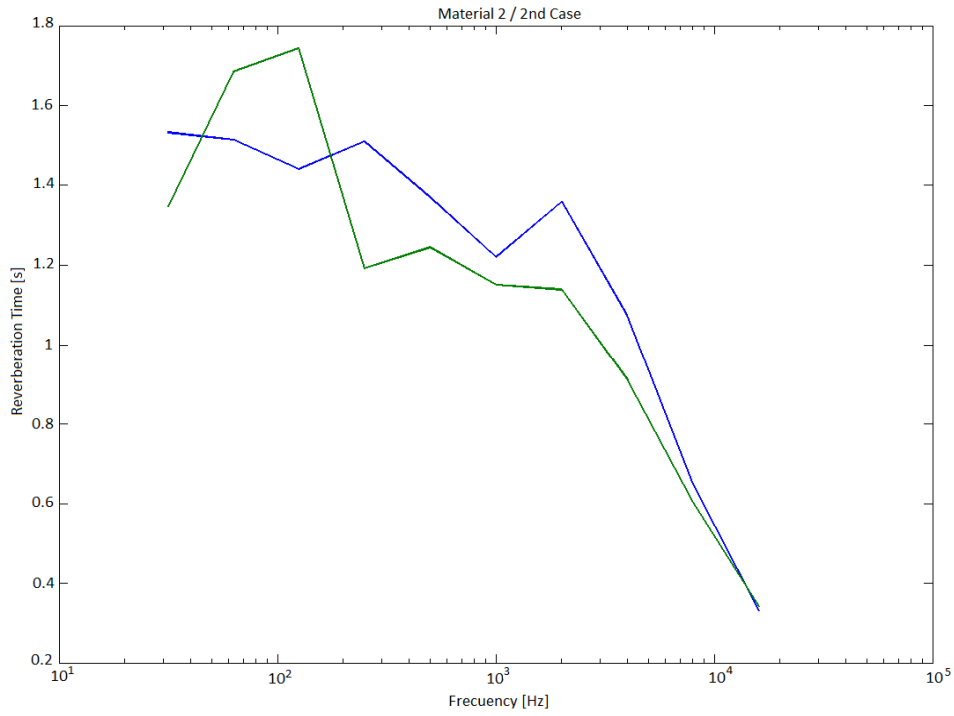


9 (c): Results for the reverberation time for the case one with $\alpha = 0.02$ and zero scattering. The graphic shows the angle-dependent (blue line) and diffused averaged (green line) modeling for material 3.

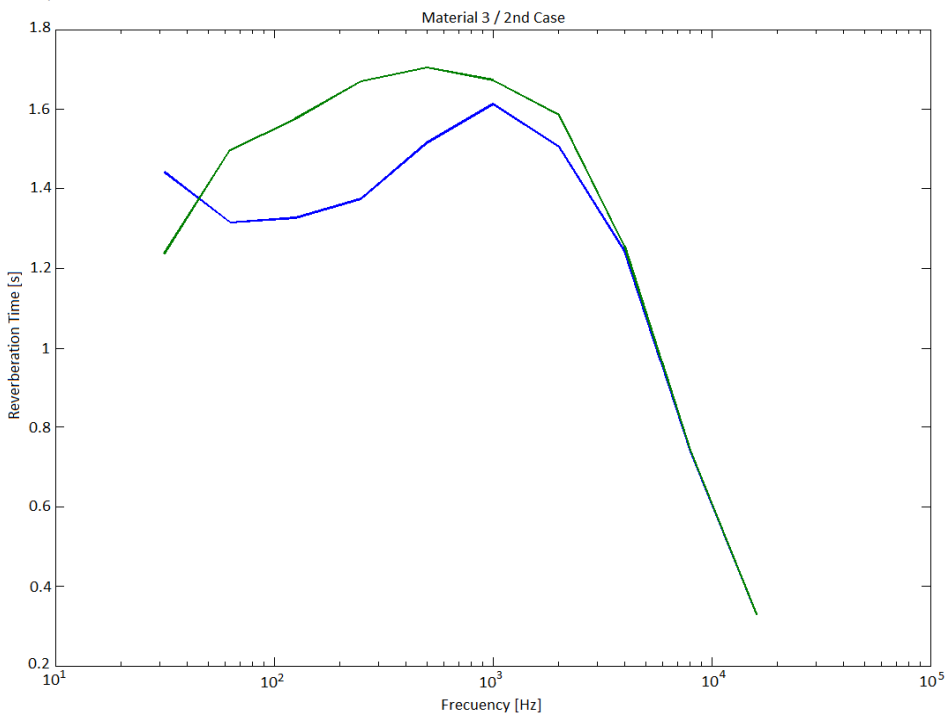


9 (d): Results for the reverberation time for the case one with $\alpha = 0.2$ and zero scattering. The graphic shows the angle-dependent (blue line) and diffused averaged (green line) modeling for material 1.

5. Discussion of results

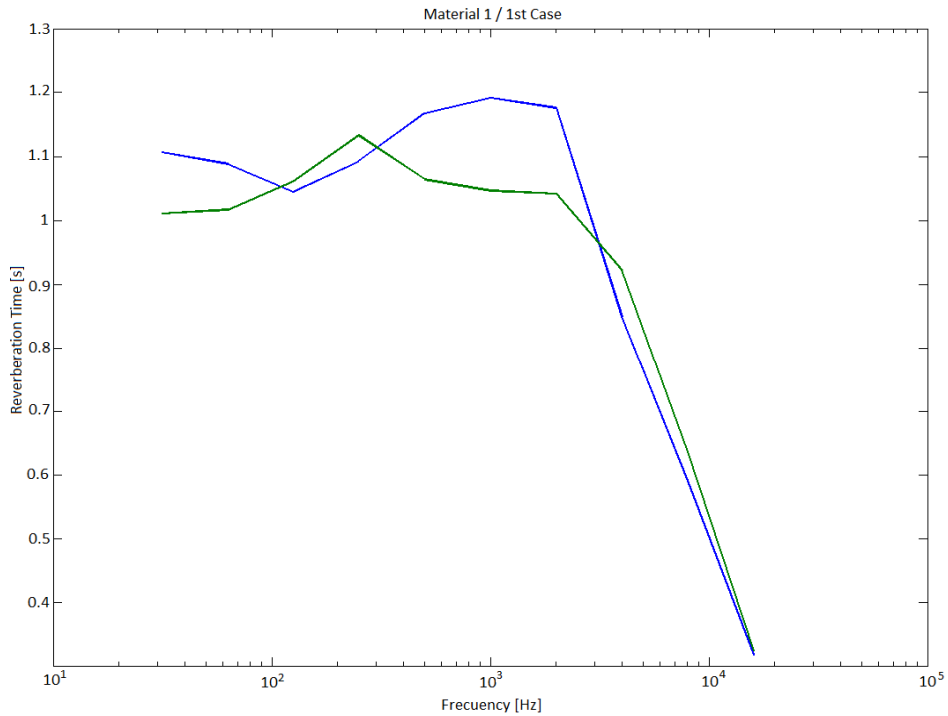


9 (e): Results for the reverberation time for the case one with $\alpha = 0.2$ and zero scattering. The graphic shows the angle-dependent (blue line) and diffused averaged (green line) modeling for material 2.

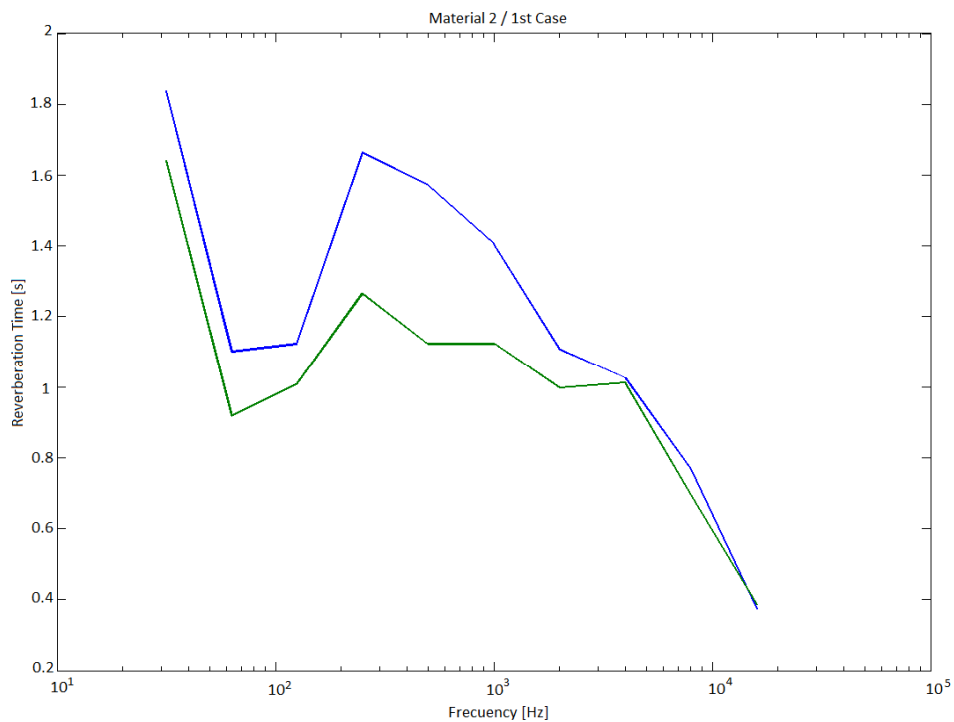


9 (f): Results for the reverberation time for the case one with $\alpha = 0.2$ and zero scattering. The graphic shows the angle-dependent (blue line) and diffused averaged (green line) modeling for material 3.

Figure 9: Results for the reverberation time for the different cases with zero scattering. Each graphic put together the angle-dependent (blue line) and diffused averaged (green line) modeling of the rear absorber with applied material. On the ordinate axe is represented the Reverberation time (T_{30}). On the abscissa axe shows the frequency in Hertz.

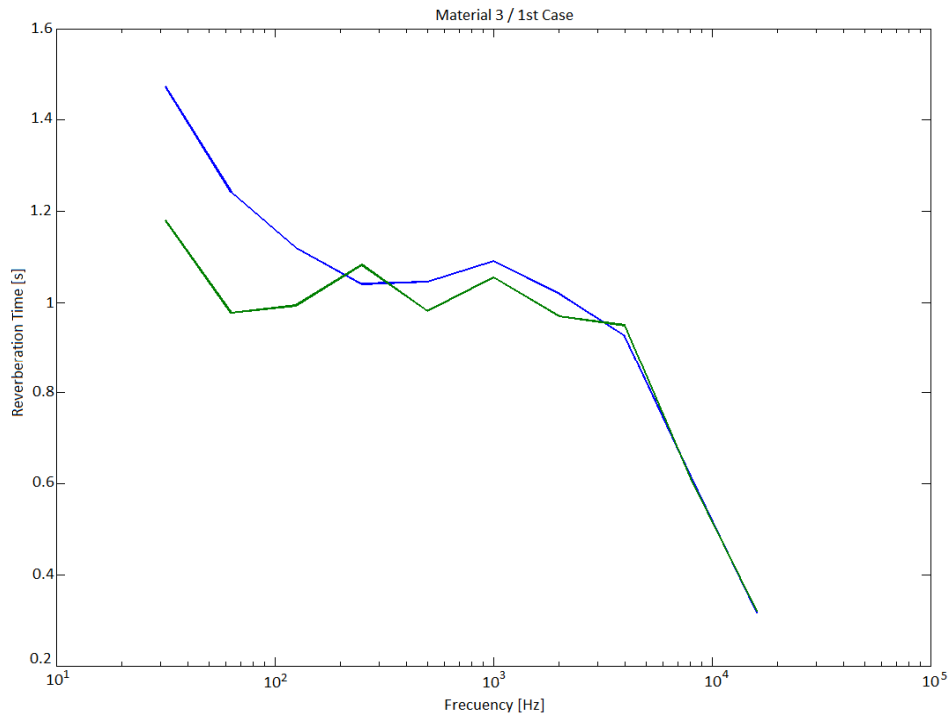


10 (a): Results for the the reverberation time for case one with $\alpha = 0.02$ and scattering 0.2. The graphic shows the angle-dependent (blue line) and diffused averaged (green line) modeling for material 1.

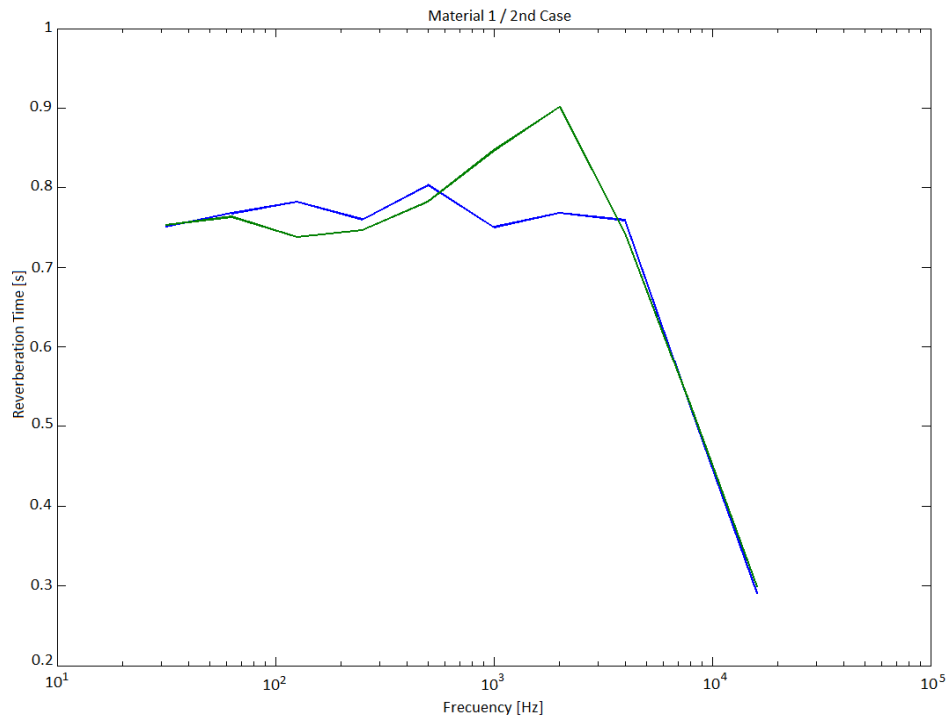


5. Discussion of results

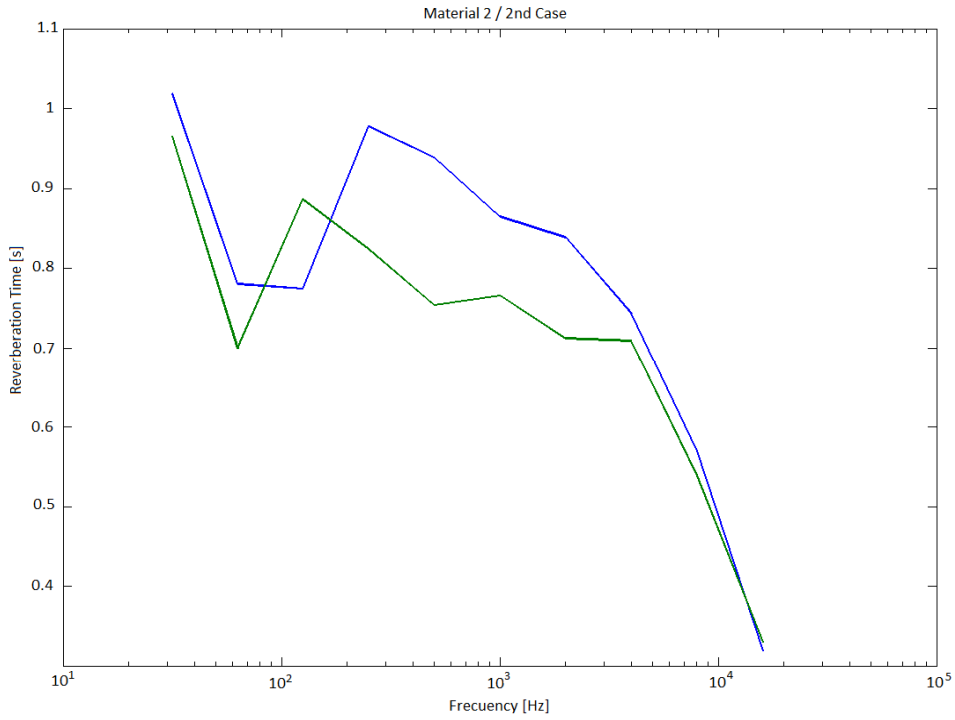
10 (b): Results for the the reverberation time for case one with $\alpha = 0.02$ and scattering 0.2. The graphic shows the angle-dependent (blue line) and diffused averaged (green line) modeling for material 2.



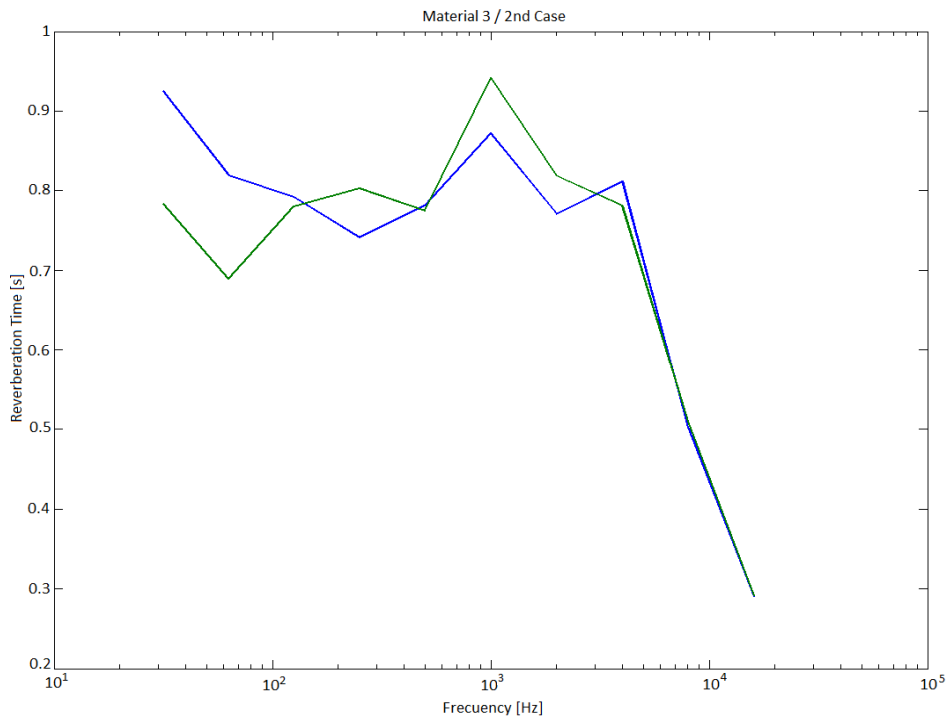
10 (c): Results for the reverberation time for the case one with $\alpha = 0.02$ and scattering 0.2. The graphic shows the angle-dependent (blue line) and diffused averaged (green line) modeling for material 3.



10 (d): Results for the reverberation time for the case one with $\alpha = 0.2$ and scattering 0.2. The graphic shows the angle-dependent (blue line) and diffused averaged (green line) modeling for material 1.



10 (e): Results for the reverberation time for the case one with $\alpha = 0.2$ and scattering 0.2. The graphic shows the angle-dependent (blue line) and diffused averaged (green line) modeling for material 2.



5. Discussion of results

10 (f): Results for the reverberation time for the case one with $\alpha = 0.2$ and scattering 0.2. The graphic shows the angle-dependent (blue line) and diffused averaged (green line) modeling for material 3.

Figure 10: Results for the different cases with a scattering value of 0.2. Each graphic put together the angle-dependent (blue line) and diffused averaged (green line) modeling of the rear absorber with applied material. On the ordinate axe is represented the Reverberation time (T_{30}). On the abscissa axe shows the frequency in Hertz.

5.2. Listening test results

The listening tests carried out for this thesis took place in the Virtual Reality Laboratory at the *Institut für Technische Akustik* (ITA). Apart from the facilities where the test was run, the individuals used Sennheiser HD 600 headphones and two different signals which alternate randomly in a three-alternative forced-choice experiment. The simulated room was a lecture hall as shown in Figure 11, with a 2200 m³ volume. The absorption coefficient was $\alpha = 0.15$ and $\alpha = 0.3$, as a main difference with the computer simulation values. Furthermore, the scenarios created, with $\alpha = 0.15$ and $S = 20\%$, were used for the listening test. Also, a new material (Material 4) was created, homogeneous porous foam of 25cm thickness. Therefore, different scenarios were created alternating the diffuse and angle-dependent implemented materials with the different scattering values. Subjects, then, listened to the convolved signal (pink noise or piano sample) trying to perceive the changes between the signal, listening to any difference. The results obtained after the listening test allowed determining the impact of the reflection model on the perceived room acoustics. The discussion focus on the changes perceived by the listeners. Due to the analysis, the conclusion will show if the assumption considered at the beginning of this work is perceived by subjects.

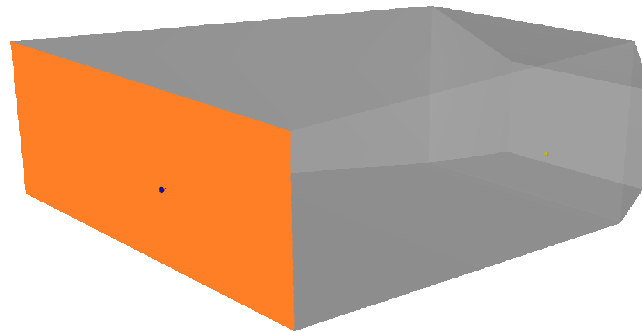


Figure 11: Lecture hall with a volume of 2200 m³. The orange wall shows where the materials were employed.

The most noticeable effects correspond to Material 2 (Figure 7), where the absorption is mainly produced in for angles below 30° -and its mirror value and high frequencies (dark blue line in the mentioned figure represents 8000 Hz). This result is empathized knowing that, according to the literature, the ear is more sensitive to high frequencies. Figure 15, where the scattering coefficient was doubled, shows that there is not a proportional change between the increase in the value and the results. It must be taken into account that perception of sound sources which contains the audible range of frequencies, compared to the natural sound signal, increases the ability of listeners to detect changes.

For the clarity the minimum value to perceive a difference between signals is 1 dB after DIN-ISO 3382 [48]. In Figure 12(b) is shown that for 3 kHz and 6 kHz the deviation is over 2 dB. For the reverberation time deviations are also produced over the 10% that is noticeable for listeners, in the same frequencies. In the fourth case, using Material 4 in the rear wall, results for the angle-dependent and diffuse-averaged properties are similar, except for very low frequencies, such as 20-30 Hz (Figure 13).

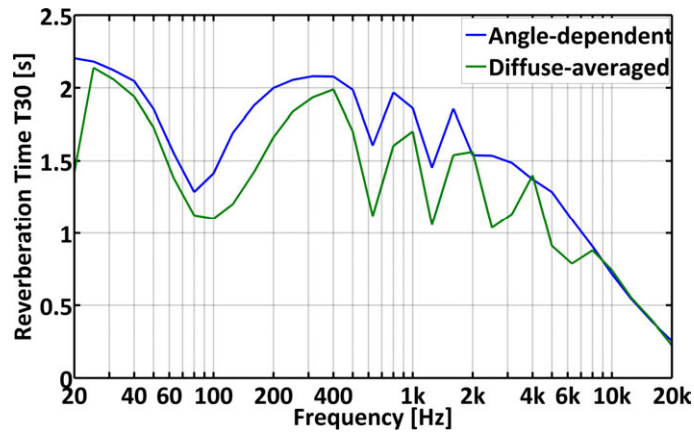


Figure 12 (a): Reverberation time of the lecture hall showing differences between diffuse and angle-dependent modeling of the rear wall absorber with applied material 2.

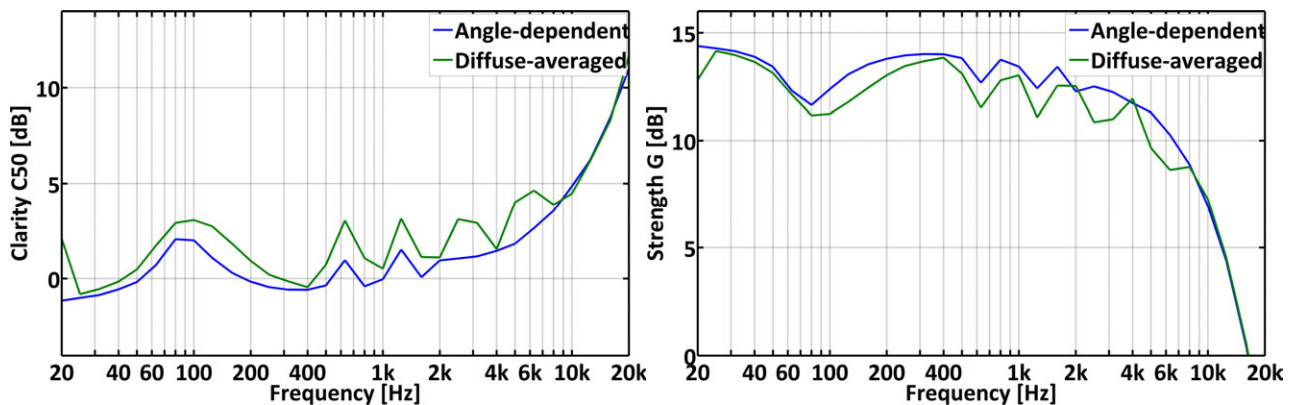


Figure 12 (b) and Figure 12 (c): Left: clarity 50 and right: strength G of the lecture hall showing differences between diffuse and angle-dependent modeling of the rear wall absorber with applied material 2.

Figure 12: Objective results of the lecture hall showing differences between diffuse and angle-dependent modeling of the rear wall absorber with applied material 2. Remaining walls were set to 15% absorption and 20% scattering.

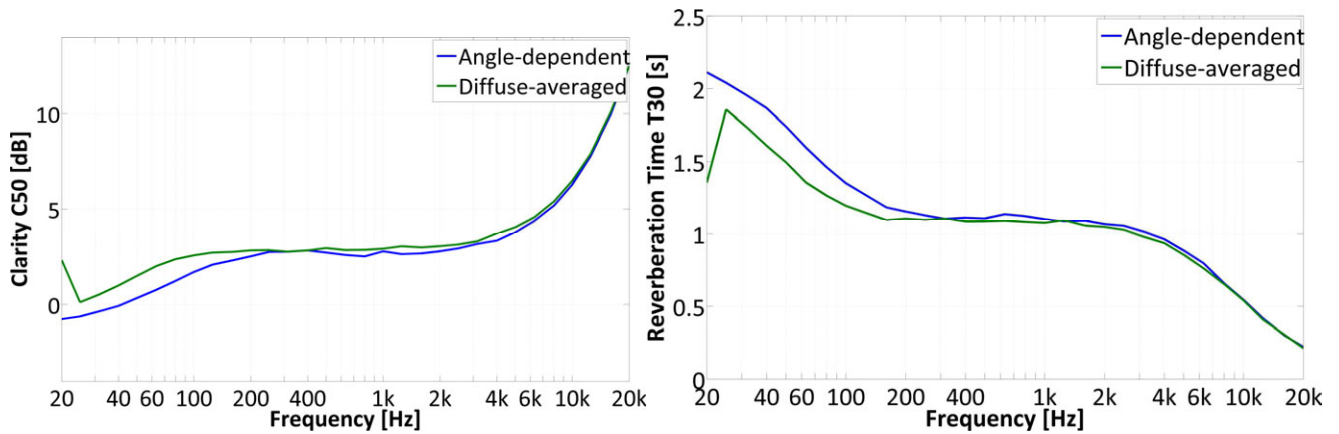


Figure 13 (a) and **Figure 13 (b)**: Left: clarity 50 and right: reverberation time of the lecture hall showing differences between diffuse and angle-dependent modeling of the rear wall absorber with applied material 4.

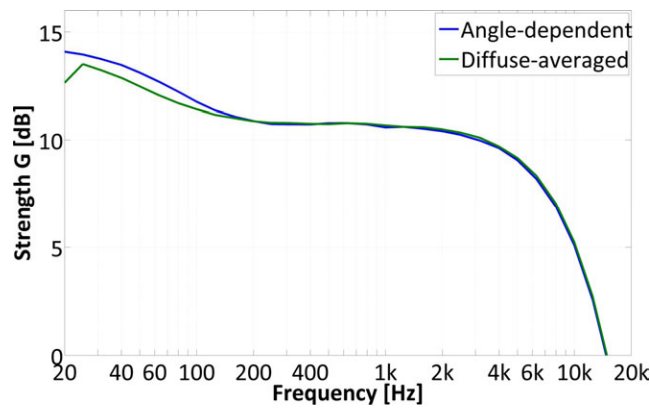


Figure 13 (c): Strength G of the lecture hall showing differences between diffuse and angle-dependent modeling of the rear wall absorber with applied material 4.

Figure 13: Objective results of the lecture hall showing differences between diffuse and angle-dependent modeling of the rear wall absorber with applied material 4. Remaining walls were set to 15% absorption and 20% scattering.

The threshold of 67% detection rate (green line draw in Figures 14, 15, 16) marks the turning point of psychometric function and thus the point of highest uncertainty between a tendency towards the ability or non-ability to detect the differences between diffuse and angle-dependent implementation. The median over all subjects and experiments resulted in a detection rate of 52% which is significantly below this threshold of 67%. It can be concluded that the majority of people tend towards not being able to detect the differences in the presented stimuli.

5. Discussion of results

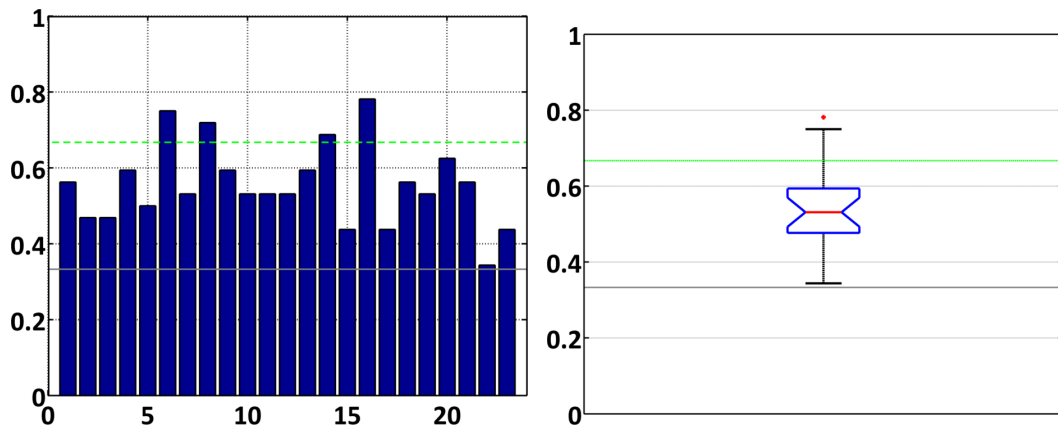


Figure 14: Results of the listening test with detection rates on the ordinate. On the left are the detection rates of all 23 participants. On the right all results are averaged. The median lies significantly below the 67%-point of the detection range.

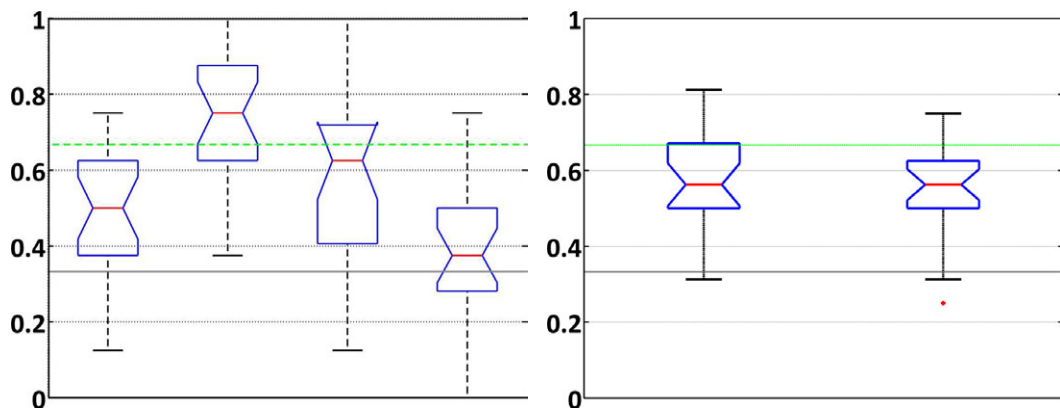


Figure 15: Results of the listening test with detection rates on the ordinate. On the left are the four different materials A, B, C and D. On the right are two different absorption coefficients (left: 30% vs right: 15%).

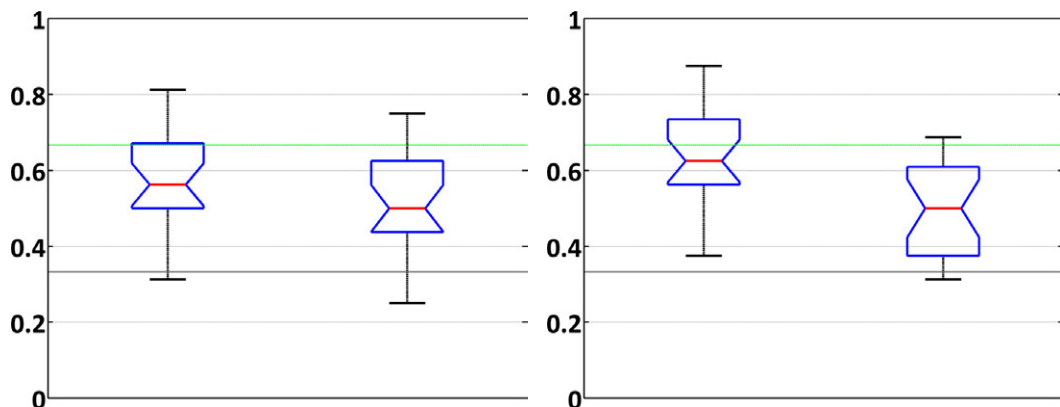


Figure 16: Results of the listening test with detection rates on the ordinate. On the left are two different scattering coefficients (left: 0% vs. right: 20%). On the right are two different signals (left: pink noise bursts vs. right: piano).

6. Conclusion

In this thesis, the evaluation of the effects of angle-dependent absorption coefficient in room acoustics simulations is discussed. Therefore, simulations were run using different materials in a box-shaped room and a hall room, to show the changes due to angle-dependent absorption coefficient. The first approaches allowed the author to get an idea of the limited literature on the subject, one of the problems to face.

It is simple to realize the implementation of angle-dependent reflection factors in geometrical acoustics simulation algorithms. As a result, there was a benefit from the advanced reflecting modeling in some special configurations. Concretely, in a sensitive test scenario with exaggerated material properties. The variations in the room acoustic parameters, due to the angle-dependent absorption coefficient, were slightly detected by listeners in the extreme cases. These extreme cases happened when the values of the diffused and absorption coefficient for the similar walls had the maximum values.

For the synthesis of angle-dependent reflection factors data, computer simulations based on the Komatsu and Mechel model were run. **Matlab** coding and **RAVEN** software were used in the computer laboratory to achieve the objective results. Materials used for each case were created by the author, according to the materials properties given by the different literature and manufacturers catalogues.

In the present case study, only in some configurations there was a meaningful response from the advanced reflecting modeling. First results obtained providing angle-dependent data lead to a new consideration in the field of room acoustics, realizing new projects in the future. It must be said that it is not expected to result in significantly audible effects if reflection modeling is done generally angle-dependent, instead of diffuse-averaged in typical scenarios. Acoustic parameters taken into account for the evaluation were clarity, reverberation time and early decay time.

On the other hand, for the subjective evaluation data, a listening test was run with a population of 23 individuals. As all of the subjects have a background in acoustics, it lets to an interpretation of the results where shows how people with a knowledge in the field had problems to identify the different cases. As a result, extrapolating the data, the study confirmed that the variation of the type of reflection modeling is hardly perceived by people.

In conclusion, the assumption of variable values for the angle-dependent absorption coefficient is proved. But the subjective response of individuals showed that there are only little changes in the perception if the coefficient varies in small differences between the values handle in the simulations. Also, if acoustics material parameters are not exaggerated, subjects do not perceive any variations.

Outlook

Further simulations with different kinds of rooms, such as the ones represented in Figure 2 and 11, and materials with different properties should be run to obtain more accurate results. These materials can give a harder statement of the objective evaluation results, given in the conclusion of this thesis, and get different cases for a wider subjective evaluation with several cases in the study. For instance: if changes are not only perceived in the extreme cases. Also, different listening test should be carried out, but using a population without a background in acoustics and set in actual rooms, so the results will show the response of potential users of the spaces. Furthermore, a higher number in the population taking the listening test will give more accurate subjective results.

Appendix A

Tafel 6.25 Längenbezogene Strömungsresistenz verschiedener Dämmschichten

Dämmschicht	Rohdichte kg/m ³	längenbezogene Strömungsresistenz 10 ³ N·s/m ⁴
Mineralfasermatten und -platten (Kamilit), kunstharzgebunden	50	10
	80	25
	110	40
	140	60
	170	80
Glasfasermatten, kunstharzgebunden, aus kurzstapeligen Fasern	25	5
	50	25
PC-Faser-Isoliermatten	100	40
Mineralfaserhartplatten	450 ... 500	500 ... 700
Faserstoffplatten aus pflanzlichen Fasern (Altmarkplatte)	220	450 ... 500
Holzwohle-Leichtbauplatten	360 ... 450	0,1 ... 1
Harnstoff-Formaldehydharzschaum (Platherm N), offenporig	15	30 ... 300
Phenol-Formaldehydharzschaum (Plastapor), gemischtporig	60 ... 80	100 ... 350
Polyurethan-Weichschaum, offenporig	25 ... 40	5 ... 30

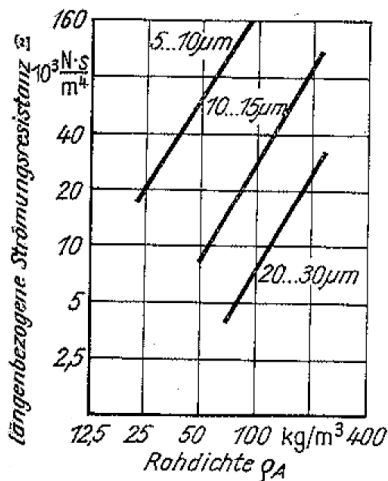


Bild 6.55 Längenspezifische Strömungsresistenzen von losen Glasfasern verschiedenen Faserdurchmessers in Abhängigkeit von der Rohdichte

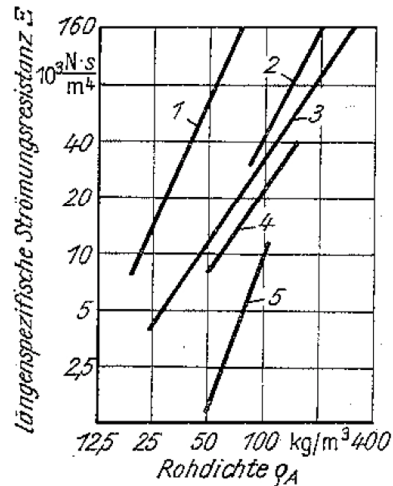


Bild 6.56 Längenspezifische Strömungsresistenzen von Fasern
1 Baumwolle; 2 PC-Fasern; 3 Mineralfaser,
2 ... 10 μm; 4 Basaltwolle, 2 ... 8 μm;
5 Aluminiumwolle, 7 μm

Figure 17: 6.25 Length-related Airflow resistivity in different layers of insulation.
6.55 Specific Airflow resistivity of loose optical fibers, multiple fiber diameter as a function of density.
6.56 Specific Airflow resistivity of fibers. 1 cotton, 2 PC-Fibers; 3 mineral fiber, 2 ... 10 μm; 4 basalt wool, 2 ... 8 μm; 5 aluminum wool, 7 μm.

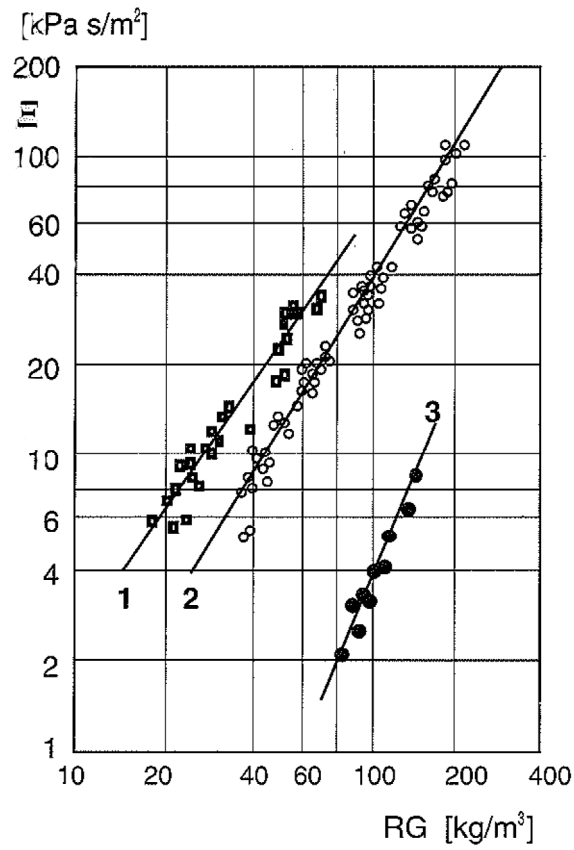


Figure 18: Strömungsresistenz ξ verschiedener Fasermaterialien als Funktion des Raumgewichts RG ; Meßpunkte und Regressionsgeraden.

- 1: Glasfaser;
- 2: Basaltwolle;
- 3: Monofile Mineralfaser.

Appendix B

Material	Composition	Features
First Material	Basaltwolle	Dicke ⁶ = 0,07 m Strömungsresistanz = 80 KPa/m ²
	Luft	Dicke = 0,17 m
	Lochplatte	Dicke = 0,07 m Loch-Radius = 0,006 m Entfernung Loch = 0,015 m
	Luft	Dicke = 0,003m

Gesamtdicke des dritten Materials = 0,32 m.

Table 7: Composition, size, characteristics and thickness of the first material describe in point 3.5.4.

Material	Composition	Features
Second Material	Lochplatte	Dicke = 0,25 m Loch-Radius = 0,055 m Entfernung Loch = 0,14 m
	Luft	Dicke = 0,17 m
	Basaltwolle	Dicke = 0,07 m Strömungsresistanz = 80 KPa/m ²

Gesamtdicke des zweiten Materials = 0,49 m.

Table 8: Composition, size, characteristics and thickness of the second material describe in point 3.5.4.

⁶ As the parameters used by the **ITA_Toolbox** are in German, all data in Tables 7, 8 and 9 are given in the same language to facilitate the user any change performed in the *ita_impcalc_gui*.

Material	Composition	Features
Third Material	Porous Material (Komatsu Model)	Dicke = 0,03 m Strömungsresistenz = 55 KPa/m ²
	Luft	Dicke = 0,005 m
	Basaltwolle	Dicke = 0,04 m Strömungsresistenz = 80 KPa/m ²
	Luft	Dicke = 0,2 m
	Lochplatte	Dicke = 0,07 m Loch-Radius = 0,04 m Entfernung Loch = 0,12 m
	Luft	Dicke = 0,005 m

Gesamtdicke des ersten Materials = 0,35 m.

Table 9: Composition, size, characteristics and thickness of the third material describe in point 3.5.4.

Bibliography

- [1] S. Pelzer, M. Müller-Trapet & M. Vorländer, “Angle-dependent reflection factors applied in room acoustics simulation”, *AIA-DAGA 2013 Conference on acoustics*, Merano, Italy, 18th-21st March.
- [2] T. Komatsu, “Improvement of the Delanz-Bazley and Miki models for fibrous sound-absorbing materials“, *Acoustical Science and Technology*, n. 2, vol. 29, pp. 121-129, 2008.
- [3] E. Mommertz, “Untersuchung akustischer Wandeigenschaften und Modellierung der Schallrückwürfe in der binauralen Raumsimulation“, *Dissertation RWTH Aachen University*, Shaker, 1996.
- [4] J. H. Rindel, “Modeling the angle-dependent pressure reflection factor”, *Applied Acoustics*, vol. 38, pp. 223-224, 1993.
- [5] T. J. Cox and P. D’Antonio, *Acoustic absorbers and diffusers. Theory, design and application*, Spoon press (Taylor and Francis Group), 1st Edition, 2004.
- [6] F. P. Mechel, *Formulas of acoustics*, Springer, 1st Edition, 2002
- [7] I. Bork, “A comparison of room simulation software. The 2nd Round Robin on room acoustical computer simulation”, *Acta Acustica united with Acustica*, vol. 86, no. 6, pp. 943-956, 2000.
- [8] M. Vorländer and E.Mommertz, “Definition and measurement of random-incidence scattering coefficients”, *Applied Acoustics*, vol. 60, no. 2, pp. 187-199, 2000.
- [9] T. Sakuma, “Approximate theory of reverberation in rectangular rooms with specular and diffuse reflections”, *Journal of the Acoustical Society of America*, vol. 132, no. 4, pp. 2325-2336, 2012.
- [10] P. D’Antonio and B. Rife, “The state of the art in the measurement of acoustical coefficients”, *Proceeding of Meetings on Acoustics*, vol. 12, p. 015008, 2011.
- [11] D. Stanzial and A. Fuschini, “Room-average absorption coefficient determination by means of intensity measurements in steady-state acoustic field conditions”, *Journal of the Acoustical Society of America*, vol. 87, Issue S1, pp. S10-S10, 1990.
- [12] F. V. Hunt, “Investigation of room acoustics by steady state transmission measurements”, *Journal of the Acoustical Society of America*, vol. 11, Issue 1, pp. 80-94, 1939.
- [13] M. Yuzawa, “A method of obtaining the oblique incident sound absorption coefficient through an on-the-spot measurement”, *Applied Acoustics*, vol. 8, no. 1, pp. 27-41, 1975.
- [14] E. Mommertz, “Angle-dependent *in-situ* measurements of reflection coefficients using a subtraction technique”, *Applied Acoustics*, vol. 46, pp. 251-263, 1995.
- [15] E. R. Kuipers, Y. H. Wijnant and A. De Boer, “A numerical study of a method for measuring the effective *in-situ* sound absorption coefficient”, *Journal of the Acoustical Society of America*, vol. 132, no. 3, pp. 236-242, 2012.

Bibliography

- [16] U. Ingård and R. H. Bolt, “A free field method of measuring the absorption coefficient of acoustic materials”, *Journal of the Acoustical Society of America*, vol. 23, no. 5, pp. 509-516, 1951.
- [17] ISO, “Acoustics - Sound-scattering properties of surfaces - Part 1: Measurement of the random-incidence scattering coefficient in a reverberation room (ISO 17497-1)”, 2003.
- [18] ISO, “Acoustics – Measurement of sound absorption in a reverberation room (ISO 354)”, 2003.
- [19] ISO, “Acoustics – Determination of sound absorption coefficient and impedance in impedance tubes – Part 1: Method using standing wave ratio (ISO 10534-1)”, 2001.
- [20] R. Otdam, S. Hoen, D. de Vries & M. Vörlander, “Measurement of angle-dependent reflection coefficients with a microphone array and spatial Fourier transform post-processing”, *Fortschritte der Akustik, AIA-DAGA*, Meran, Italy, 2013.
- [21] A. Omoto, “Comment on ‘A theoretical Framework for quantitatively characterizing sound field diffusion based on scattering coefficient and absorption coefficient on walls’”, *Journal of the Acoustical Society of America*, vol. 133, no. 1, pp. 9-12, 2013.
- [22] F. Dierkes, “*Winkelabhängige Reflexionsfaktoren: Messmethoden und Anwendung in der Auralisation* (Angle-dependent reflection factors: Measurement methods and application in auralization)”, *Diplomaufgabe*, Institut für Technische Akustik RWTH-Aachen, May 2012.
- [23] P. V. Brüel, *Sound insulation and room acoustics*, Chapman and Hall, Ltd., 1st Edition, 1995.
- [24] Y. Takahashi, T. Otsuru and R. Tomiku, “*In situ* measurements of absorption characteristics using two microphones and environmental ‘anonymous’ noise”, *Acoustical Science and Technology*, n. 6, vol. 24, pp. 382-385, 2003.
- [25] C.-H. Jeong, “Guideline for Adopting the Local Reaction Assumption for Porous Absorbers in Terms of Random Incidence Absorption Coefficients”, *Acta Acustica United with Acustica*, vol. 97, pp. 779-790, 2011.
- [26] R. Lanoye, G. Vermeir and W. Lauriks, “Measuring the free field acoustic impedance and absorption coefficient of sound absorbing materials with a combined particle velocity-pressure sensor”, *Journal of the Acoustical Society of America*, n. 5, vol. 119, pp. 2826-2831, 2006.
- [27] C. Nocke, “In-situ acoustic impedance measurement using a free-field transfer function method”, *Applied Acoustics*, n. 59, pp. 253-264, 2000.
- [28] T. J. Cox, “Acoustic iridescence”, *Journal of the Acoustical Society of America*, n. 3, vol. 129, pp. 1165-1172, 2011.
- [29] M. E. Delany and E. N. Bazley, “Acoustical properties of fibrous absorbent materials”, *Applied Acoustics*, n.3, pp.105–116, 1970.

- [30] Y. Miki, “Acoustical properties of porous materials - Modifications of Delany-Bazley models”, *Journal of the Acoustical Society of America*, Japan (E), n. 11, pp. 19–24, 1990.
- [31] L. L. Beranek, *Journal of the Acoustical Society of America*, n.13, pp. 248, 1943.
- [32] J. Redondo, R. Picó, M.R. Avis and T.J. Cox, “Prediction of the Random-Incidence Scattering Coefficient Using a FDTD Scheme”, *Acta Acustica united with Acustica*, vol. 95, no. 6, pp. 1040-1047, 2009.
- [33] J. H. Rindel, “Computer simulation techniques for the acoustical design of rooms - how to treat reflections in sound field simulation”, *ASVA 97*, Tokyo, pp. 201-208, 2-4 April 1997.
- [34] U. Ingard, *Noise reduction analysis*, Jones and Bartlett Publishers, LLC, 1st Edition, 2010.
- [35] C. Hopkins, *Sound insulation*, Elsevier Ltd, 1st Edition, 2007.
- [36] E. Brandão, P. Mareze, A. Lenzy and A. R. da Silva, “Impedance measurement of non-locally reactive samples and the influence of the assumption of local reaction”, *Journal of the Acoustical Society of America*, vol. 133, no. 5, pp. 2722-2731, May 2013.
- [37] J. B. Allen and D. A. Berkley, “Image method for efficiently simulating small-room acoustics”, *Journal of the Acoustical Society of America*, vol. 65, no. 4, pp. 943-950, April 1979.
- [38] H. Kuttruff, *Acoustics: An introduction*, Taylor & Francis, 2007.
- [39] M. Vorländer, *Auralization. Fundamentals of acoustics, modeling, simulation, algorithms and room buildings*, Springer, RWTH Edition Colection, 1st Edition, 2008.
- [40] M. Förster, “*Auralization in room acoustics*”, Bachelor’s thesis, Institute of Broadband Communications Graz University of Technology, Graz, July 2008.
- [41] Nordtest, “NT ACOU 11 - Acoustics: Human sound perception – Guidelines for listening tests”, *Northtest method*, 2002-2005.
- [42] H. Levitt, “Transformed Up-Down Methods in Psychoacoustics”, *Journal of the Acoustical Society of America*, vol. 49, no. 1, pp. 467-477, 1971.
- [43] Head acoustics, “Conducting listening tests”, Application note.
- [44] C. C. Wier, W. Jesteadt and D. M. Green, “A comparison of method-of-adjustment and forced-choice procedures in frequency discrimination”, *Perception & Psychophysics*, vol. 19, no. 1, pp. 75-79, 1976.
- [45] Prof. Dr.-Ing. Wolfgang Fasold, Prof. Dr.-Ing. habil. Wolfgang Kraak & Dr.-Ing. Werner Schirmer, *Taschenbuch akustik. Teil 2*, pp. 913, chap. 6.4.1. Poröse Schallabsorber, Veb Verlag Technik Berlin, 1.Auflage, 1984.
- [46] F. P. Mechel, *Schallabsorber. Band II: Innere Schallfelder und Strukturen*, pp. 113, chap 6.3 Stömungsresistenz, S. Hirzel Verlag Stuttgart, 1. Auflage, 1995.
- [47] ISO, “Acoustics -- Measurement of room acoustic parameters - Part 2: Reverberation time in ordinary rooms (ISO 3382-2:2008)”, 2008.

